C. W. THORNTHWAITE ASSOCIATES
LABORATORY OF CLIMATOLOGY

EVALUATION OF AN OCEAN TOWER FOR THE STUDY OF CLIMATIC FLUXES

by

C. W. Thornthwaite, W. J. Superior
and R. T. Field

Technical Report No. 2, Contract Nonr 2997(00)
NR 389-101, Office of Naval Research

Final Report, Contract No. N62306-1122
U.S. Naval Oceanographic Office

Centerton, New Jersey
December 1962

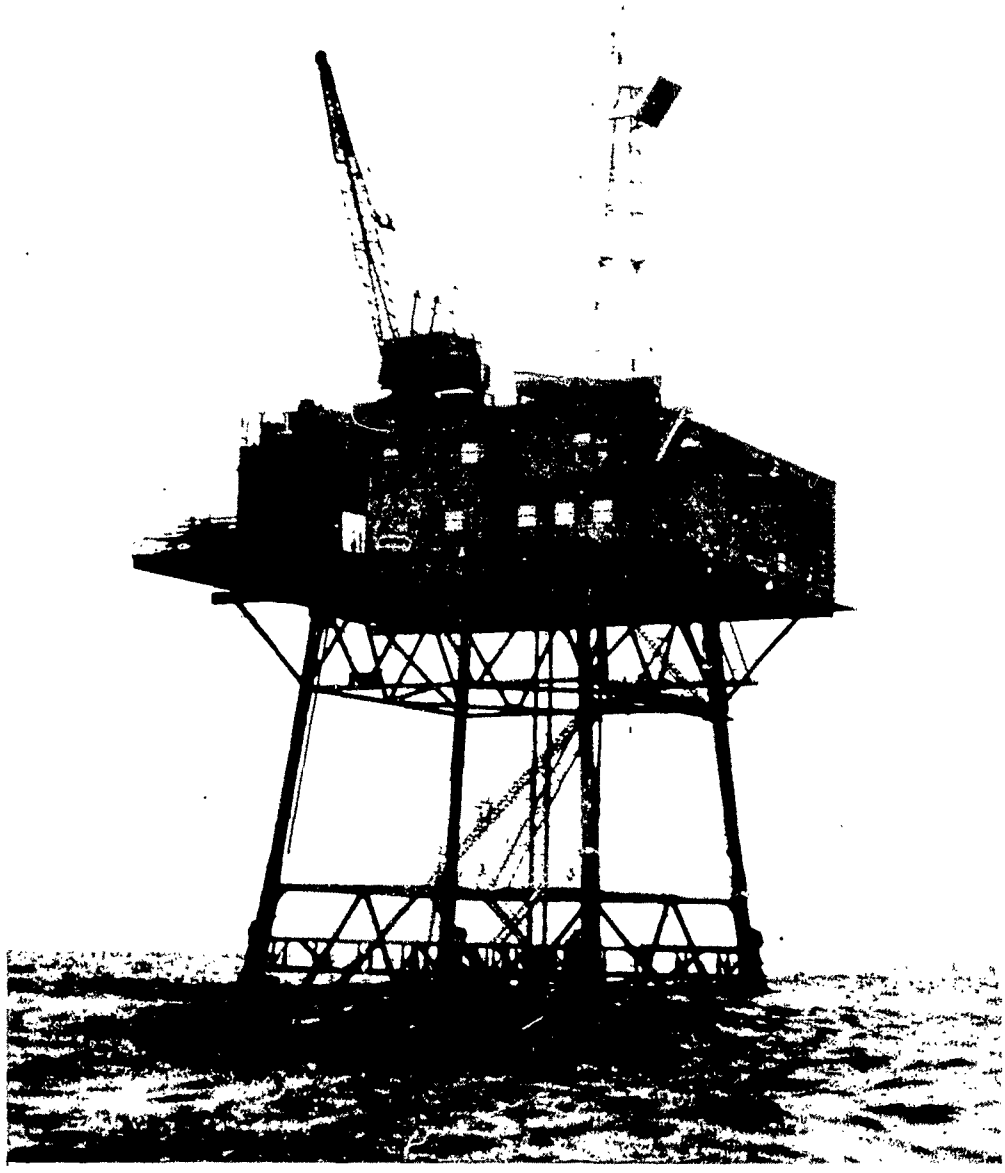

C. W. THORNTHWAITE ASSOCIATES
LABORATORY OF CLIMATOLOGY

EVALUATION OF AN OCEAN TOWER FOR THE STUDY OF CLIMATIC FLUXES

by

C. W. Thornthwaite, W. J. Superior
and R. T. Field

Technical Report No. 2, Contract Nonr 2997(00)
NR 389-101, Office of Naval Research

Final Report, Contract No. N62306-1122
U. S. Naval Oceanographic Office

Centerton, New Jersey
December 1962

FINAL REPORT, CONTRACT NO. N62306-1122
U. S. NAVAL OCEANOGRAPHIC OFFICE

TECHNICAL REPORT NO. 2, CONTRACT NONR 2997(00)
NR 389-101, OFFICE OF NAVAL RESEARCH

The research reported in this document has been sponsored in part by the U. S. Naval Oceanographic Office under Contract No. N62306-1122, and in part by the Department of the Navy, Office of Naval Research, under Contract No. Nonr 2997(00), NR 389-101.

TABLE OF CONTENTS

INTRODUCTION

The earth's surface is very complex, being made up of a disordered mosaic of land and water, forest and clearing, trees, bushes, hedgerows and buildings. The annual budgets of water and energy are highly affected by these surface differences. Small variations in roughness, reflectivity, plant-cover or wetness may produce large differences in water and energy exchanges above the surface. The dubious present state of boundary layer theory does not allow us to compute these differences: so we have to measure them. Hence we must possess instruments sensitive enough to measure the rapid fluctuation involved, strong enough to stand up to use in the field, and unobtrusive enough not to influence the element to be observed by their own presence. Hitherto we have lacked such instruments.

Much of the present work in micrometeorology involves the so-called aerodynamic approach to determine the turbulent exchange of momentum, heat, and moisture between the surface and atmosphere. This method requires measuring the gradients of wind velocity, temperature, and atmospheric moisture near the surface, and involves manipulations of these gradients according to the semi-empirical aerodynamic theory to obtain momentum, heat, and water vapor fluxes.

It is generally agreed that adequate gradient observations can be obtained only over extensive, flat, open unobstructed terrain. Without a sufficiently extensive unobstructed fetch, the turbulent transfer processes are not in equilibrium adjustment with the ground surface throughout the wind profile. Wholly adequate exposures are the exception over most natural land surfaces. However, the open ocean provides the ideal wind fetch. It would appear, therefore, that the ideal place to assess the energy and moisture budgets would be over the relatively homogeneous ocean surfaces. Many attempts have been made to obtain the necessary measurements from ships, and thought has been given to using fixed platforms to support instrumentation. Unfortunately, ships and platforms interpose obstacles that interfere greatly with the unobstructed airflow that is sought for study. Ships and platforms so modify the vertical gradients of velocity, moisture, and heat that existing aerodynamic theory cannot be expected to yield accurate values of the vertical energy and moisture fluxes. In spite of this, the need for observations is so great that many different research groups have instrumented ships and towers and used them to collect the limited flux data which we now have for the oceans.

The U. S. Naval Oceanographic Office (formerly the U. S. Navy Hydrographic Office) has for the past several years conducted an oceanographic research program on one of the Texas Tower installations off the east coast of the United States. Because of the importance of both oceanographic and micrometeorological research in the vast ocean areas of the world, the office has been seeking to expand these research studies. Various tower sites have been studied and in 1961 the Argus Island tower located some 30 miles southwest of Bermuda was selected as the site for further micrometeorological investigations. Argus Island as shown in

the frontispiece is a fixed platform on a steel tower. It is essentially a box approximately 85 feet on a side and 25 feet high with its floor about 72 feet above the water. The structure offers much obstruction to the wind, and therefore, it was doubted that reliable vertical profiles of wind, temperature, and humidity could be obtained from it. Accordingly, considerable thought was given to the erection of a separate structure removed from Argus Island for the express purpose of obtaining meteorological information.

In November 1961 the Hydrographic Office circulated a letter to a selected group of research scientists who had been working on problems of flux measurements over different surfaces asking for their advice and suggestions. A portion of the original request for advice is given below:

> "The Hydrographic Office is instrumenting an oceanographic-meteorological research platform aboard Argus Island Tower located on Plantagenet Bank southwest of Bermuda . . . one phase of this program will concentrate on a study of the energy exchange between the sea and the atmosphere. Experience has shown the inadequacy of Texas Tower-type platforms in studies concerning transfer of momentum, heat, and water vapor, due to interfering effects of the tower . . . Therefore, to fulfill the increasing demand for reliable measurements relevant to these studies, it is planned to initiate construction of a specially designed structure (a Wand) from which observations of the vertical distribution of wind velocity, temperature, and humidity can be made. This structure will be located in the immediate proximity of Argus Island but far enough away so that the measurements will not be appreciably affected by the presence of the tower."

In a later evaluation of the comments concerning the possible use of a wand, the stated objectives of the research program were given as

> "a) to study the method by which energy is transferred from the atmosphere to form ocean waves, (b) to gain basic information concerning the structure of the atmosphere adjacent to the sea surface, and (c) to study the flux of heat and water vapor, etc. in the atmosphere immediately above the ocean surface."

In reviewing the possible use of a meteorological wand to be set up at some distance from Argus Island, various research scientists pointed out a number of problems concerning instrumentation, the great difficulty in servicing the instruments, the possible influence of the bulk of the wand itself on the atmospheric environment, the lack of stability of the wand and the influence of its motion on the sensors, and the problems of the present aerodynamic approach.

Our own group has worked with the aerodynamic approach for more than twenty-five years in an effort to increase our knowledge of the energy and moisture

fluxes at the earth's surface. Some of the original profile studies were undertaken by Thornthwaite and Holzman (1939, 1940) in Arlington, Virginia on the present site of the Pentagon Building. Recognizing the limitations of the method, we have sought other ways to determine fluxes near the surface. We have recently developed some new instrument systems for measuring atmospheric fluxes and have used them to make measurements of the fluxes of momentum, heat, moisture, and ozone in connection with Government-sponsored research studies. Our experience with the new method suggested that it might be feasible to obtain good flux measurements from a platform such as Argus Island itself, since the observations do not involve vertical profiles of wind but are made at one level only. If it were verified that the desired fluxes and other meteorological information can be obtained by instruments exposed from the platform itself, the entire micrometeorological research program could be greatly simplified and its cost would be much less.

While the ultimate objective of a micrometeorological research study at Argus Island is to determine the energy and moisture exchange at the sea surface, it was recognized that it would first be necessary to assess the magnitude and extent of the disturbance which the platform introduces in the wind flow. Moreover, attention had to be given to problems of mounting instruments away from the structure if it were determined that useful flux measurements might be obtained. A preliminary contract was proposed which would enable us to visit Argus Island and take observations in various places around it.

Specifically, a contract with the U. S. Naval Oceanographic Office was entered into on August 11, 1962 to:

a) obtain sufficient observations to construct the wind flow pattern around the platform on Argus Island tower;

b) determine whether routine observations of the vertical flux of momentum, sensible heat, and moisture could be obtained from, but not influenced by, the tower structure;

c) recommend sites for location of sensors and indicate the limitations of the sites.

This preliminary study was to be completed by November 1, 1962.

In order to complete the work required, field teams were sent to Argus Island during August, September and October 1962 and numerous wind, temperature and radiation data were obtained. The present report sums up our preliminary conclusions concerning the micrometeorological conditions around the platform, our recommendations for its future use in studying the fluxes of energy and moisture over the surface of the ocean, and some of our recent experience with flux measurements over land.

SURVEY OF WIND FLOW ON ARGUS ISLAND

The assigned task of this contract was to conduct an on-the-spot survey of wind flow around Argus Island. Although it is nothing more than a box approximately 85 feet on a side and 25 feet high with its floor about 72 feet above the water, the wind flow around it is exceedingly complex. Ideally to determine the wind flow around this structure we should install several hundred anemometers and operate them simultaneously in various locations. Since such a program was impractical, it became necessary to move the available instruments from one location to another. The survey employed four men on three trips for a total of 42 days of residence on the platform. The first trip occurred during the calm summer weather of mid-August, the second during the hurricane season of September and the third in the stormy autumn weather of late October.

At the beginning of the survey a single sensor was installed on the top of the microwave tower to serve as a reference for comparison of the various observations. This reference anemometer is hereafter referred to as "the tower reference" and the wind speed recorded from it is denoted by $\bar{u}_T$. The natural wind varied greatly in speed and direction from one set of observations to another. In order to compare observations taken in one location with high wind with others obtained somewhere else with low wind, all velocities were reduced to ratios to the reference velocity observed at the same time. Throughout the survey all measurements were compared with the corresponding simultaneous tower reference velocity.

Since the various appendages to the platform, the structures and objects upon and under it, interfere strongly with the wind, the pattern of interference will vary with wind direction. Accordingly, there was no possibility of combining observations taken with the wind in different directions. During the August trip the wind remained steadily from the south and established the pattern for the survey. The wind was more variable in September and October, but on each trip there were some periods with south wind. The analysis that follows gives the flow pattern around the platform when the wind is from the south.

It was hoped that so long as the wind direction remained constant the ratio of the wind velocity at a point of observation to the reference would be independent of velocity. This was found to be true at the exposed sites to the windward. To the leeward, as would be expected even small variations in direction from south resulted in substantial changes in the ratios. Above the platform, near the deck the ratios varied widely but away from the deck the ratios were constant with velocity. Below the platform the supporting structures imposed such a complex pattern of interference that the ratio varied considerably with direction, velocity and time. Nevertheless, all of the observations were converted to ratios and were plotted on a cross section of the platform.

Study of the distribution of the ratios around the platform made it quickly apparent that this did not give an indication of the interference which the platform produced. Rather, what was wanted were the ratios of the wind velocity at the points of observation to the velocities at those levels if the platform had not been there.

The vertical profile of the wind over the sea follows the familiar logarithmic law so long as the thermal structure of the air is adiabatic. The entire profile can be established by means of measurements at only two levels. When the friction parameter, z_0, is known a wind velocity measurement at one level will give the profile. Thirty years ago, Rossby (1932) made a detailed study of the frictional force between air and water and gave some estimates as to the probable value of z_0. In summary in a later paper (1936) he said:

> "In the case of rapidly changing conditions, the roughness may reach very high values ($z_0 \approx 20$ cm), but with steady winds the sea surface appears to adjust itself in such a fashion as to permit the air to move over it in the most economical fashion. The roughness parameter corresponding to steady moderate to strong winds seems to be in the vicinity of 0.6 cm."

Rossby's assigned value of 0.6 cm for z_0 was adopted in a series of studies on evaporation from the ocean, made in this country by Sverdrup (1937, 1940), Montgomery (1940) and Jacobs (1942). Roll in Germany obtained many determinations of z_0 over the sea by making observations of wind profiles (1948, 1948a, 1949). His values are much lower than Rossby's estimate, ranging between .002 cm and .006 cm. He later (1951) revised the value upward to a range between .009 cm and .352 cm. Deacon and his associates (1956) gave a range between 0.05 cm and 0.15 cm and Brocks (1959) gave 0.2 cm.

We have adopted a value for z_0 that is accordant with the later determinations and about one order of magnitude smaller than Rossby's suggested value. Our value s .078 cm (.003 ft). Using this value of z_0 and unit velocity at the reference level we have computed the wind profile according to the logarithmic law. It is given in table 1.

During most of the observation periods a recording was made of the temperature difference between 150 ft and 23 ft above mean sea level, which showed that neutral or very nearly neutral conditions prevailed the whole time. Thus, it is valid to compare the actual wind observations with the theoretical values given in table 1 to determine where the wind has been slowed down by the obstruction and where it has been speeded up. The result of this comparison is given in figure 1.

Figure 1 locates by means of Cartesian coordinates the more than 150 points of observation used to determine the wind flow around the structure. The averages used in compiling this diagram are given in Appendix III which summarize the actual observations assembled in Appendix II. Wind velocity observations were

Table 1

Vertical Distribution of Wind over the Sea Assuming a Logarithmic Wind Profile, Unit Velocity at Reference Level and z_0 = .003 ft.

z (ft)*	u''_z/u''_R**	z (ft)	u''_z/u''_R	z (ft)	u''_z/u''_R
150	.937	98	.900	46	.834
148	.936	96	.898	44	.831
146	.934	94	.896	42	.826
144	.933	92	.894	40	.822
142	.932	90	.892	38	.818
140	.931	88	.890	36	.813
138	.930	86	.888	34	.808
136	.928	84	.886	32	.803
134	.927	82	.884	30	.797
132	.926	80	.882	28	.791
130	.924	78	.880	26	.785
128	.923	76	.878	24	.778
126	.922	74	.876	22	.770
124	.920	72	.873	20	.762
122	.919	70	.871	18	.753
120	.917	68	.868	16	.743
118	.916	66	.866	14	.731
116	.914	64	.863	12	.718
114	.913	62	.860	10	.702
112	.911	60	.857	8	.683
110	.910	58	.854	6	.658
108	.908	56	.851	4	.623
106	.907	54	.847	2	.563
104	.905	52	.844	1	.503
102	.903	50	.841	0.5	.443
100	.902	48	.838	0.003	.000

* Distance in feet above mean sea level.

** Ratio of undisturbed wind velocity to velocity at reference level.

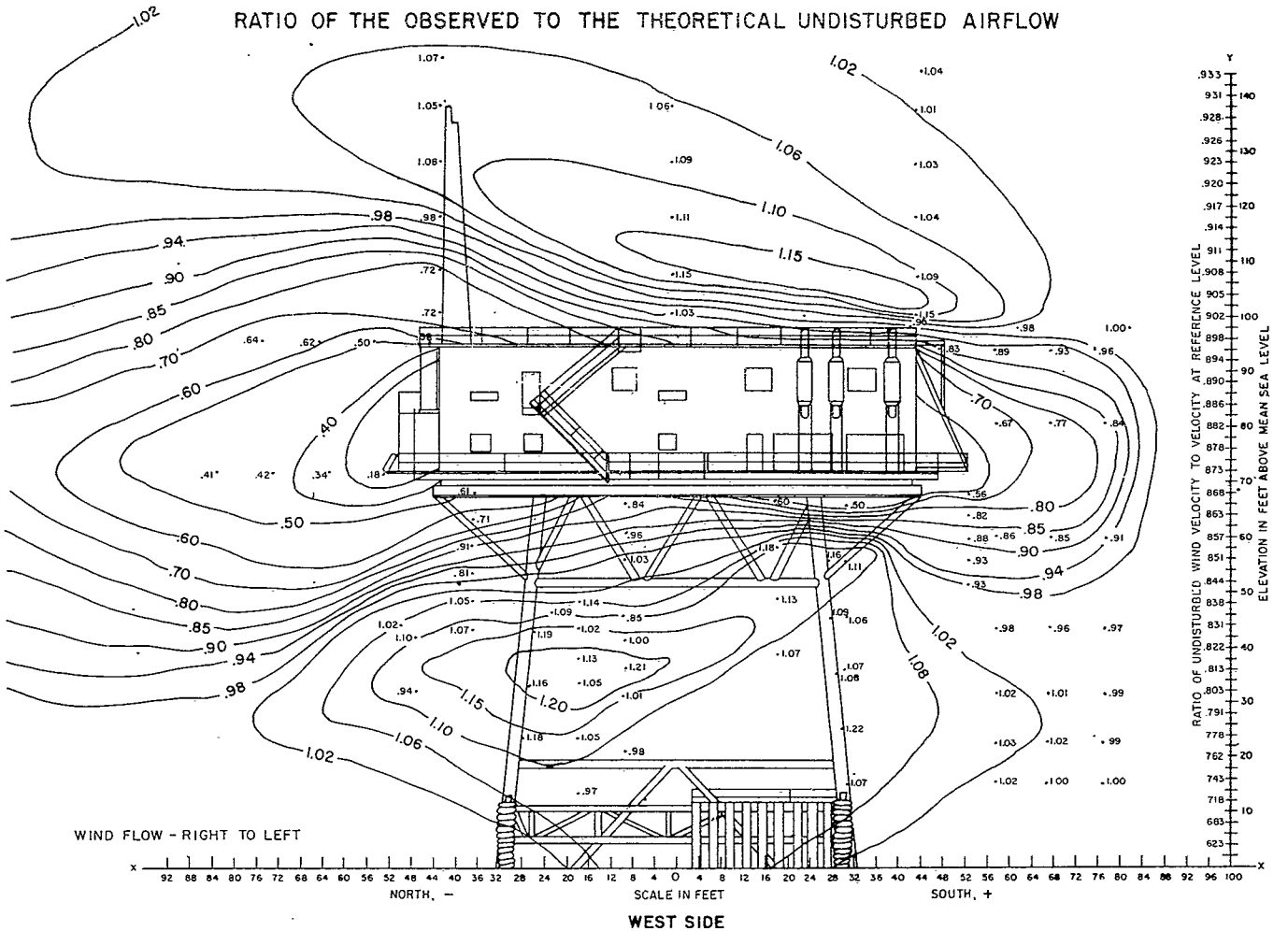
RATIO OF THE OBSERVED TO THE THEORETICAL UNDISTURBED AIRFLOW
WIND FLOW - RIGHT TO LEFT
NORTH, −
SCALE IN FEET
SOUTH, +
RATIO OF UNDISTURBED WIND VELOCITY TO VELOCITY AT REFERENCE LEVEL
ELEVATION IN FEET ABOVE MEAN SEA LEVEL
WEST SIDE

Figure 1

made as near as was feasible to a plane bisecting the platform from north to south. Figure 1 represents the disturbed flow in two dimensions moving from right to left. The disturbance field is expressed at each observational point by means of the ratio between normalized observed and theoretical velocities

$$\frac{\bar{u}_z}{\bar{u}_T} \Big/ \frac{u''_z}{u''_R}$$

where $\bar{u}_z$ is the observed wind speed at a point, $\bar{u}_T$ is the simultaneous tower reference speed, u''_z is the theoretical undisturbed wind speed at height z and u''_R is the undisturbed speed at a selected reference level z_R. Values of the ratio u''_z/u''_R are given in the tabulated logarithmic wind profile in table 1.

The tower reference anemometer, operated simultaneously with all observations, was installed above the microwave tower at coordinate position (-42, 147). The other observations were made with four to six anemometers mounted on a two inch diameter, hardened aluminum tubing mast assembly. Since the tubing weighed only 4.2 lbs per 12 ft section and required only a minimum of guying, it proved quite easy to position anemometers temporarily as far away as 50 to 60 ft from the structure. Three or more ten minute runs were completed at each mast location before moving to a new position. At most positions three runs proved sufficient to produce statistically stable averages; occasionally more runs were necessary. At some positions beneath and in the lee of the platform the wind speed was highly sensitive to changes in wind direction as small as 10° to 20°. Observations to windward did not appear to be so sensitive. Appendix II gives the actual speeds measured around the tower and their ratio to the simultaneous tower reference speed.

To permit meaningful analysis, it was necessary that the tower reference speed bear a known relation to the undisturbed flow. It had been hoped at the outset of the study that the wind measured at (-42, 147), fifty feet above the deck, would represent undisturbed flow and could provide the required reference speeds. However, during the study it became apparent that one would have to go either much higher or farther upwind to find undisturbed flow. During the October visit an effort was made to compare the wind speed at the tower reference with flow which was presumed to be much less disturbed. A 50 ft mast was erected to position vertical and horizontal anemometers over the south face of the tower at (43, 145). The data of this comparison are presented as runs A-E at the end of Appendix II. For a period of 250 minutes, with winds 7-8 m sec^{-1} from 215° the ratio of the speed to the tower proved to be .971, indicating a 3 percent difference in wind speed at the two points. However, the air flow at this new position also proved to be somewhat disturbed, since the vertical anemometer there measured a 19:1 ratio of updrafts to downdrafts during the test. Consequently, none of the observation points could be adopted with any assurance that it be free of disturbance. It was necessary to approach the problem indirectly. It was done in the following manner.

It was known from the test described above that the observed speeds at the tower reference (-42, 147) for south winds were at least 1.03 times the undisturbed flow, and probably higher still. It was thought that the disturbed speed at (43, 145) might be about 1.04 times the undisturbed speed. This would make the speed at the tower reference approximately 1.07 times the undisturbed speed. Accordingly, a theoretical logarithmic profile with $z_0 = .003$ ft was constructed through the tower reference level (147 ft) such that the theoretical speed at 147 ft equaled .935 times the speed at the theoretical profile reference level. The profile reference is then the height at which the undisturbed wind speed in a logarithmic profile equals the disturbed tower speed. This is the profile presented in table 1. The ratios of normalized wind speed to the normalized theoretical profile speeds were then plotted at each observational point in figure 1. The resulting pattern of the disturbed wind field gives a reasonable distribution of accelerated and retarded flow around the platform. That the pattern shows an approximately equal distribution of accelerated and retarded flow is taken as confirmation that the theoretical profile adopted is a good approximation of the real undisturbed profile.

Figure 1 shows that the wind speed is retarded in front of and behind the vertical wall of the platform, to less than 50 percent and 20 percent respectively of the theoretical value. The wind speed is also retarded in rather shallow layers above and below the platform. Most striking are two jets of higher wind speed which have developed above and below the platform. The upper jet develops wind speeds more than 15 percent above the theoretical and the lower one wind speeds more than 25 percent above theoretical. The disturbed condition of the wind extends far downwind of the platform, beyond the reach of any possible measurements during the survey. Above the platform the disturbance extends upward from the deck at least 50 feet and probably more than 100; and beneath it, down to the sea surface. On the windward side, however, the wind flow is relatively undisturbed (within plus or minus two percent) beyond about forty feet of the platform. Sixty feet upwind the flow would appear to be little affected by the existence of the platform. This is an inference that will have to be verified by later additional observations.

It is to be expected that any other vertical plane parallel to the one of figure 1 would display essentially the same air flow. Thus, what appear as two jets on figure 1 are actually two air layers which have been compressed and thus speeded up. A scattering of observations taken on the east and west sides show that the disturbance to the air flow there is about the same as above and below, giving a similar pattern of greater and lower wind speeds. Accordingly, it is our conclusion that reliable observations for making flux determinations can be made from the windward face of the structure, but nowhere else.

It would be impossible without making further measurements to state quantitatively the reliability of the disturbance pattern revealed in figure 1. A number of questions remain to be answered. The most basic of them relate to the assumed theoretical profile. What is the influence of wind speed and wave height on z_0? Is the logarithmic wind profile a good representation of the real profile at heights of 50, 100 and more feet above the ocean surface? None of the data now in hand can begin to answer these questions.

However, the data in Appendix II ought to reveal something of how changes in wind speed would affect the pattern in figure 1. If the observed ratios $\overline{u}_Z/\overline{u}_T$ are a function of wind speed, grouping them to construct a wind field would not be valid. That they are not, at least on the upwind portion of the structure, is shown by plotting the speed measured at a point against the tower reference speed. Figures 2, 3, and 4 show a constant relationship between tower reference wind speed and the speed measured at various upwind positions. The graphs for positions (43, 145) and (43, 116) in figure 2 include a range of tower wind from 246 to 826 cm sec^{-1}. These two positions, although not close together, show very similar and constant ratios between measured and tower velocities. However, the points for runs 8-10, positions (43, 119) and (43, 139), represent the situation for winds in excess of 10 m sec^{-1}. These last points do not appear to lie on the same line as the lower winds. The apparent discontinuity which occurs in the vicinity of 8-9 m sec^{-1} shows the tower reference velocity increasing more rapidly than at the lower speeds. Probably this reflects increased disturbance at the tower anemometer at higher speeds and different wind directions. It is to be expected that the size of the regions with accelerated and retarded flow would change with wind speed. Accordingly, at low velocities the reference may have recorded less disturbed flow.

In figure 3 there is an insufficient range of velocities to be sure of the relationship at lower speeds. However, since the fitted lines for positions (81, 99) and (61, 99) pass through the origin there is little likelihood of important discontinuities at lower winds. The air is accelerated to approximately the same degree through these points for all wind speeds. On the other hand, the three locations (76, 82), (66, 82) and (57, 82), which are located half way up the platform's windward face, exhibit quite different behavior. Although the range of speeds is too small to be conclusive, none of the three fitted lines passes through the origin. If these curves are extrapolated for low speeds to pass through the origin, they must become concave upward. If the values of $\overline{u}_Z$ at these three locations reach zero simultaneously with the values of $\overline{u}_T$, the extrapolated curves imply that the ratio $\overline{u}_Z/\overline{u}_T$, and hence the degree of disturbance, increases somewhat with wind speed. Therefore, it might be expected that the region of retarded flow will grow outward as wind speed increases.

Figure 4 shows that the disturbance near the water upwind of the platform ought to be quite independent of wind speed since the fitted lines pass through the origin. The scatter at position (76, 17) is evidence of greater random variation in wind speed as one approaches the water surface.

In the lee of the tower the random variations are too great to allow forming any conclusions about changes in the region of downwind disturbance. Above the leeward edge the disturbance seems to grow upward with increasing velocities, as is suggested in figure 5. It appears that the jet over the platform becomes constricted at lower winds say, below 8 m sec^{-1} so that the reference anemometer is in less disturbed air. Figure 6 presents the disturbance pattern over the platform for some observations of low velocity winds made in August. These observations could not be fitted with those at higher speeds shown in figure 1. This fact, plus the likelihood that the intensity of the disturbance at the reference anemometer depends somewhat on wind speed suggested that a different theoretical profile would yield a better representation of the low velocity disturbance field. A profile based on a z_o of .003 ft and the assumption that the tower reference wind speed was 1.04 times the undisturbed speed produced the low speed disturbance field shown in figure 6. The jet revealed for 5 m sec^{-1} winds is more compact than was found for higher speeds, however, the relative accelerations near the center are some 5 percent higher than those in figure 1. Nonetheless, the overall pattern is quite similar. Consequently, we conclude that the important features of the upwind disturbance pattern, its dimensions and relative magnitude, are relatively insensitive to wind speed and minor changes in wind direction. Although figure 1 is a composite of numerous measurements made under different conditions, it appears to be a good approximation of the flow pattern for the range of velocities (5-12 m sec^{-1}) represented.

DETERMINATION OF ATMOSPHERIC FLUXES

Formulation of Atmospheric Flux Equations

The measurement of atmospheric fluxes requires a method for determining the rate at which the property of the air under investigation is being transported through a horizontal plane toward and away from the earth's surface. Nearly half a century ago W. Schmidt invoked the analogy between ordinary molecular diffusion and diffusion by turbulent eddies to write a series of flux equations utilizing a coefficient of eddy diffusion or an exchange (Austausch) coefficient and the vertical gradient of the property being investigated. In general form, the equation is

$$F_s = -A \frac{d\bar{s}}{dz}$$

A being the Austausch coefficient which is related to the diffusion coefficient K, by $A = \rho K$. The preferred form of the flux equation is

$$F_s = -\rho K \frac{d\bar{s}}{dz}$$

The derivation has been applied specifically to vertical fluxes of momentum or Reynolds stress, sensible heat, and water vapor. It has recently been used in

RELATION BETWEEN $\overline{U}_Z$ AND $\overline{U}_T$ FOR POSITIONS ABOVE THE WINDWARD EDGE OF THE PLATFORM

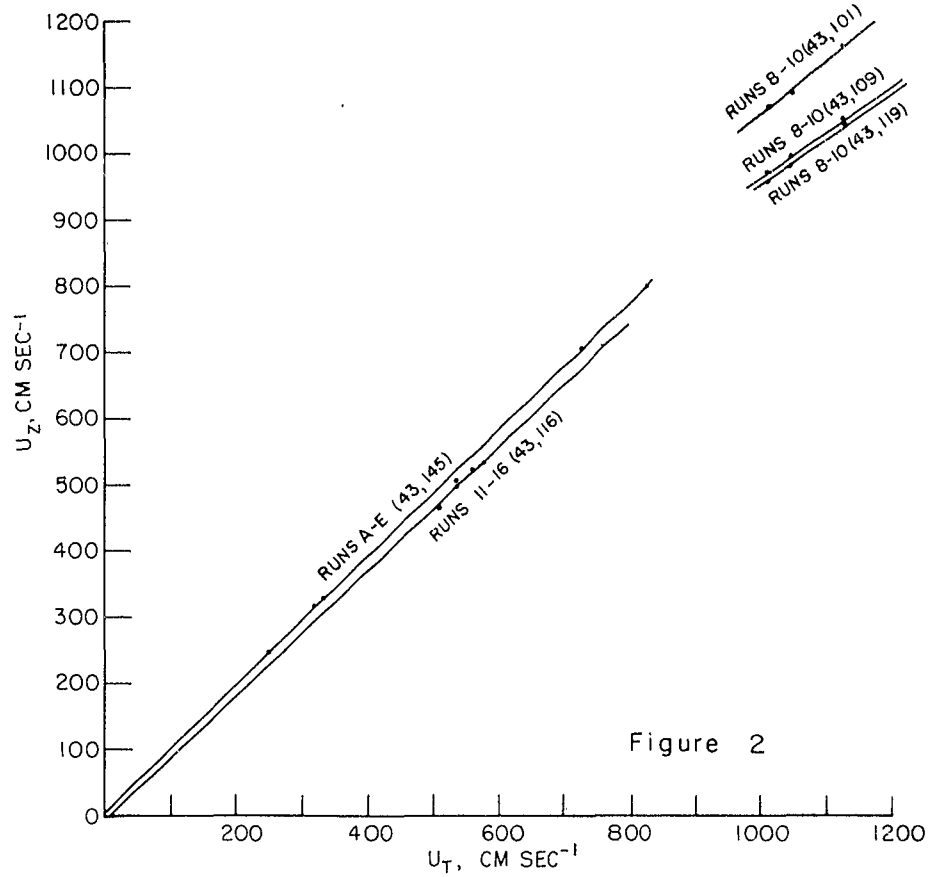

Figure 2

RELATION BETWEEN U_Z AND U_T FOR FIVE POSITIONS UPWIND OF THE PLATFORM

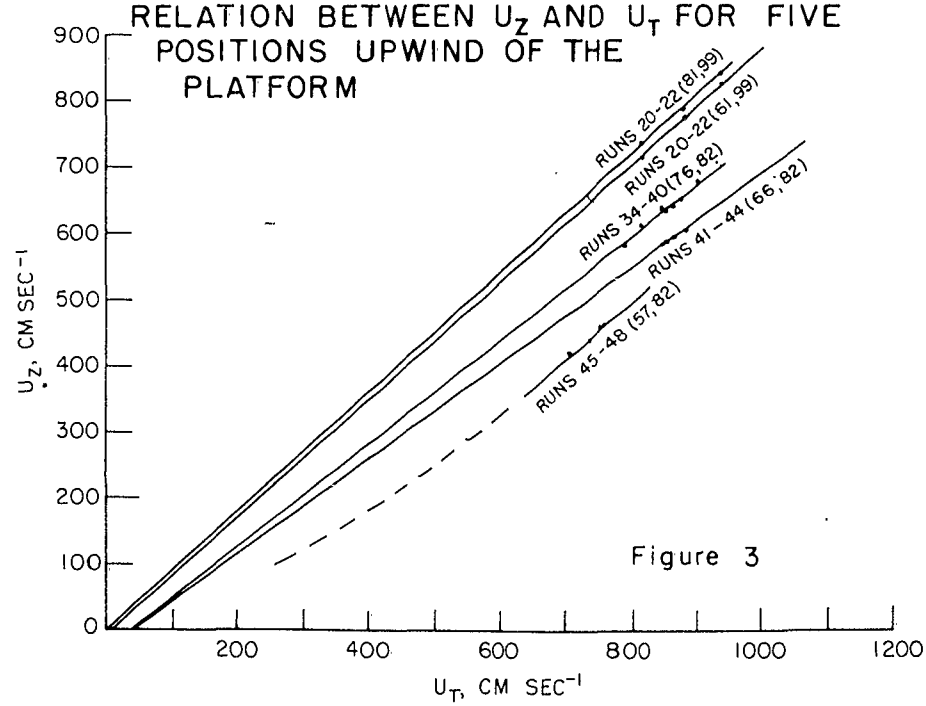

Figure 3

RELATION BETWEEN U_Z AND U_T FOR TWO WINDWARD POSITIONS BELOW PLATFORM LEVEL

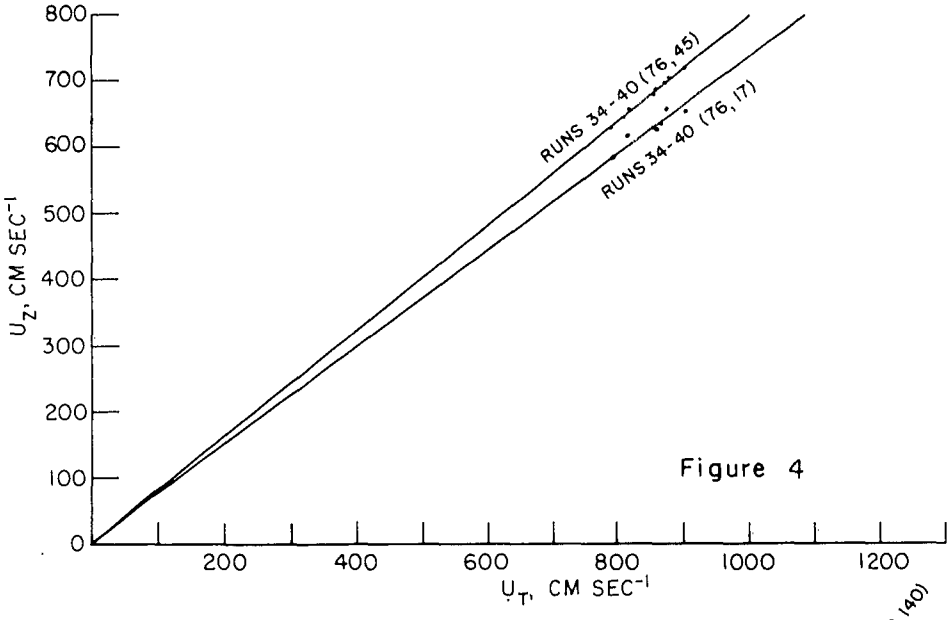

Figure 4

RELATION BETWEEN U_Z AND U_T FOR THREE POSITIONS ABOVE LEEWARD EDGE OF PLATFORM

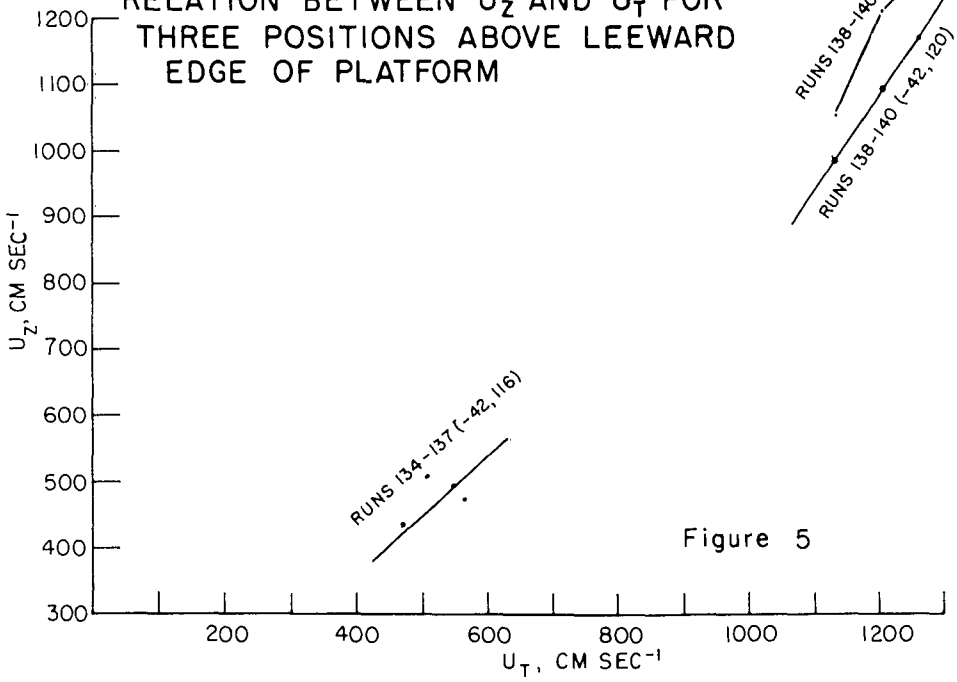

Figure 5

RATIO OF THE OBSERVED TO THE THEORETICAL UNDISTURBED AIRFLOW
LOW VELOCITY SITUATION

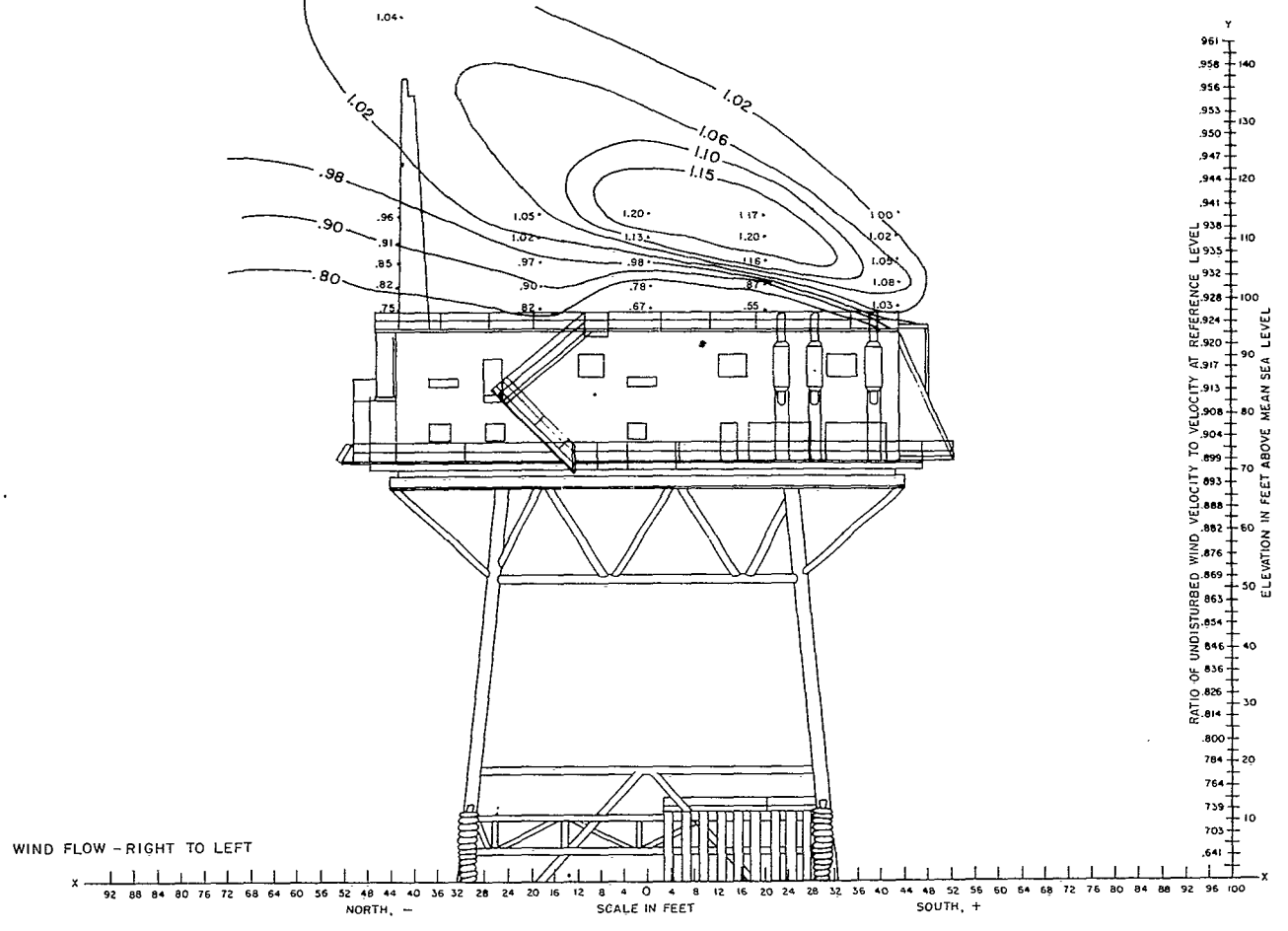

WEST SIDE

Figure 6

studies of the vertical fluxes of carbon dioxide and ozone and, of course, the diffusion coefficient, K, is itself fundamental in diffusion studies of air pollution.

Although Brunt (1952) and Geiger (1951) more than ten years ago revealed much of the confusion and uncertainty regarding K, there has not yet been any great clarification of the time and space variation of the diffusion coefficient. In recent studies of low level wind gradients, Lettau (1950, 1957) and Blackadar (1959) have reached different conclusions as to the distribution of K as a function of height and time of day. Priestley (1959) has pointed out that K increases with unstable and decreases with stable stratifications, but not according to any simple general rule. He asks for more measurements.

The familiar approach to an expression for K is due to Prandtl who sought a practical means of determining the Reynolds stress, as given by

$$\tau = -\overline{\rho w'u'}$$

where w' and u' are the vertical and horizontal components of eddy velocity. These quantities represent the deviations of the instantaneous velocities w and u from their mean values $\bar{w}$ and $\bar{u}$, as defined by $w' = w - \bar{w}$, $u' = u - \bar{u}$. What is required is a method for expressing $\overline{w'u'}$ in terms of measurable quantities. To this end Prandtl introduced the parameter l, called the mixing length.

If a parcel of air having mean velocity $\bar{u}$ is transferred upward through a distance λ to a new environment where the mean velocity is $u + \lambda \frac{du}{dz}$ and its initial mean velocity is preserved in the new environment, it follows that

$$u' = \bar{u} - (\bar{u} + \lambda \frac{d\bar{u}}{dz}) = -\lambda \frac{d\bar{u}}{dz}$$

In the absence of actual observations, it was assumed that equal amounts of kinetic energy are associated with all three eddy velocity components u', v', and w'. Thus Prandtl concluded that w' must, like u', on the average, be proportional to the distance λ, through which the turbulent eddies travel and to $\frac{d\bar{u}}{dz}$, so that w' is related to $\lambda \frac{d\bar{u}}{dz}$ although not necessarily equal to it. It can be given as $w' = a \lambda \frac{d\bar{u}}{dz}$. Remembering that u' and w' are opposite in sign, the Reynolds stress equation can be written

$$\tau = \overline{\rho (\lambda \frac{d\bar{u}}{dz})(a \lambda \frac{d\bar{u}}{dz})} = \overline{\rho a \lambda^2 (\frac{d\bar{u}}{dz})^2}$$

When λ is replaced by l, which is the mean length appropriate to both vertical and horizontal eddy velocities, defined as

$$l = \lambda \sqrt{a}$$

Prandtl's solution becomes

$$\tau = \rho l^2 \left(\frac{d\bar{u}}{dz}\right)^2$$

Recalling Schmidt's formulation for the shearing stress, the Austausch coefficient, A, may be expressed

$$A = \rho l^2 \left(\frac{d\bar{u}}{dz}\right)$$

and the diffusion coefficient is

$$K = \frac{A}{\rho} = l^2 \frac{d\bar{u}}{dz}$$

The parameter, l, was not measurable, and thus the solution was not very useful until a means could be found to determine it. Von Karman suggested a means by assuming geometrical similarity for all three components of the flow pattern. This assumption results in the relation

$$l = k_o \left(\frac{d\bar{u}}{dz} / \frac{d^2\bar{u}}{dz^2}\right)$$

where k_o is a dimensionless constant of proportionality now known as von Karman's constant. When the vertical wind gradient follows the logarithmic law, $z = z_o a^u$, this relation simplifies to

$$l = k_o z$$

By substitution we obtain

$$\tau = \rho (k_o z)^2 \left(\frac{d\bar{u}}{dz}\right)^2$$

Differentiation of the logarithmic law of the vertical wind distribution yields

$$\frac{d\bar{u}}{dz} = \frac{\bar{u}_2 - \bar{u}_1}{z(\log_e z_2 - \log_e z_1)}$$

Substitution of this expression for $\frac{d\bar{u}}{dz}$ will give the familiar expression for the shearing stress, due to Thornthwaite and Holzman (1939, 1942)

$$\tau = \frac{\rho k_o^2 (\bar{u}_2 - \bar{u}_1)^2}{(\log_e \frac{z_2}{z_1})^2} \qquad (1)$$

The above mathematical development involves assumptions and simplifications which have proved to have only restricted validity in the atmosphere. A most troublesome difficulty is associated with thermal stratification and the

stability structure of the atmosphere. The logarithmic wind profile is valid only during neutral lapse rates. When the lapse rate is unstable, the profile deviates in one direction and with stable stratification, the deviation is in the opposite direction. Similarly, the assumption of equipartition of kinetic energy among the three components of eddy velocity, u', v', and w' does not stand up. Thus, the mixing length, l, in the horizontal is not the same as the length in the vertical. The ratio of vertical length to horizontal length varies with atmospheric stability. It diminishes as stability increases. Furthermore, the length, l, is not dependent on height, z, alone but varies with velocity, u, and with stability. A necessary further condition that the shearing stress, τ, does not vary with height near the ground is not fulfilled.

Thus the work of the last two decades has involved trying to introduce corrections or revisions that would give an exchange coefficient in terms of the vertical gradient of a measurable parameter.

Rossby and Montgomery (1935), Holzman (1943) and Halstead (1943) early tried to obtain a correction by introducing an additional operator which would reduce the diffusion coefficient, K, when the atmosphere is stable and increase it when the temperature stratification is unstable. All were empirical redefinitions: the one offered by Holzman has been generally preferred (Deacon, 1949).

Since 1959 there have been three noteworthy attempts to develop satisfactory wind profile equations. These have rested on theoretical arguments which purport to account for the curvature of the diabatic wind profile. Kao (1959) argued that the friction velocity, u_*, under diabatic conditions may be represented as a function of the heat flux and u_* for neutral conditions. He then derived an expression for the wind profile which, in the first approximation, is equivalent to the /logarithmic + linear/ profile equation of Monin and Obukhov. This expression may be manipulated to yield equations for u_* and the heat flux that require measurements of only the wind velocity at three levels.

$$u_* = \sqrt{\tau/\rho} = k_o\left[\frac{(\bar{u}_2-\bar{u}_1)(z_3-z_2)-(\bar{u}_3-\bar{u}_2)(z_2-z_1)}{(z_3-z_2)\log_e z_2/z_1-(z_2-z_1)\log_e z_3/z_2}\right] \qquad (2)$$

where k_o is von Karman's constant. Knowing u_*, K_m, the eddy viscosity, may be obtained since

$$K_m \frac{d\bar{u}}{dz} = u_*^2$$

Swinbank (1960) has suggested an expression for u_* which employs the characteristic length, L, from similarity theory.

$$u_* = \frac{k_o(\bar{u}_2-\bar{u}_1)}{\log_e\left[\frac{1-e^{z_2/L}}{1-e^{z_1/L}}\right]} \qquad (3)$$

L may be evaluated from wind observations at three levels as follows:

$$\frac{\bar{u}_2 - \bar{u}_1}{\bar{u}_3 - \bar{u}_2} = \frac{\log_e\left[\frac{1-e^{z_2/L}}{1-e^{z_1/L}}\right]}{\log_e\left[\frac{1-e^{z_3/L}}{1-e^{z_2/L}}\right]}$$

Both Kao and Swinbank have attempted to introduce corrections in stability by taking account of the curvature of the wind gradient. Although the two equations have been derived along different lines of reasoning, and differ in form, they appear to give almost identical results. Both of them are highly sensitive to experimental error in the measured wind profile and demand the most careful experimental technique and optimum observational sites. Of the two, Kao's is to be preferred, on practical grounds, since it is much the easier to solve.

Panofsky (1962) (see also Panofsky, Blackadar, and McVehil, 1960) has introduced an equation for the wind profile which corrects the neutral profile by a factor derived from the Richardson number. His equation requires knowing the roughness parameter z_o, the velocity at one level, and the Richardson number, Ri, for which the vertical gradients of both wind velocity and temperature are needed. The derivation is based on similarity theory employing the Monin-Obukhov stability parameter z/L'.

$$u_* = \frac{k_o V}{\log_e z/z_o - \psi(z/L')} \tag{4}$$

where k_o is von Karman's constant

$$\psi(z/L') = \int_o^{-z/L'} \frac{1 - \varphi(z/L')}{z/L'} \, d(z/L')$$

in which

$$\varphi(z/L') = \frac{k_o z}{u_*} \cdot \frac{d\bar{u}}{dz} = \zeta$$

and z/L' is a function of Richardson number

$$z/L' = \varphi(z/L')\, Ri$$

ζ and z/L' are related by the interpolation formula

$$\zeta^4 - \zeta^3 - 18\, z/L' = 1$$

Panofsky's equation when used to determine K_m should not be so sensitive to experimental errors in the profile; however, z_o must be carefully determined under neutral conditions and must be assumed constant with velocity and stability. Also, since the Richardson number requires temperature and velocity differences between two levels the wind flow must be little disturbed at those levels.

In the meantime, various statistical theories of turbulence have been developed, following G. I. Taylor in 1921, and Sutton in 1932 and 1934. In general, these theories have attempted to define diffusion in terms of correlation coefficients and standard deviations of motions which are separated in time from one another. Sutton (1953) compares the eddies in a turbulent fluid with the molecules in a gas, "in that the motion of a particle will be the result of its encounter with various eddies, but 'eddy' is now merely a convenient way of describing a fluctuation of velocity associated with a certain scale of length." The length, l, that appears in the statistical theories is analogous to the mixing length of Prandtl, but here the concept of mixing is not essential; rather, the length refers to eddy size. It is called the scale of turbulence and represents the average size of the eddies or length scale of the fluctuations, but without implying any definite model of an eddy. All turbulence, and especially that of natural winds, is a complex of motions covering a great range of length scales, varying from those associated with the fluctuations which contain most of the energy of the motion to those typical of the very small eddies which are responsible for the ultimate dissipation of the energy into heat. (Sutton, p. 93)

This had led to the definition of the diffusion coefficient, K,

$$K = \overline{(u'^2)}^{1/2} \, l \qquad (5)$$

where the fluctuations and the length, l, are defined in statistical terms. In this formulation the measurements are of the horizontal wind.

Application of New Instrumentation

Our group has recently developed new instruments for the direct measurement of the horizontal and vertical wind which we have been able to incorporate into new systems for determining the diffusion coefficient, K, and for measuring the fluxes of momentum as well as of sensible heat and atmospheric humidity. These instruments have been described in detail (Thornthwaite, 1961; Thornthwaite, Superior, Mather, and Hare, 1961). The anemometer cups for sensing the wind speed are of lightweight molded plastic mounted by means of stainless steel spokes on an aluminum hub. The shaft to which the hub is attached carries a shutter at its lower end so as to interrupt a beam of light from a miniature lamp to a photocell housed in the horizontal anemometer support. The photocell forms a small signal which is amplified and used to actuate an electromechanical counter, each revolution of the cup assembly registering one count.

The sensor of the vertical wind anemometer is a windmill type rotor which is mounted so as to rotate in a horizontal plane. The rotor assembly, like the cup assembly, weighs only seven grams. It rotates in one direction with updrafts and in the opposite direction with downdrafts, and its rate of rotation is proportional to the vertical wind speed. The sensor distinguishes updrafts from downdrafts by use of a second photocell. Thus, upcounts and downcounts can be directed to their respective counters.

The new vertical anemometer has been designed to give a linear response to the vertical component of the wind for various angles of attack. Thus, the rate of rotation of the anemometer shaft is proportional to the instantaneous vertical velocity and each complete revolution of the shaft represents a definite distance of air travel in the vertical direction. It can be used in association with a ratemeter circuit to give a record of the actual instantaneous vertical velocity. Alternatively, a count of shaft revolutions will give time average values of the upward and downward vertical components. Thus $|\overline{w}|$ may be obtained from

$$|\overline{w}| = \frac{cr}{t}$$

where c is the response coefficient of the sensor and r is the number of revolutions in time t. These two systems are respectively called the vertical velocity anemometer and integrating vertical anemometer systems; they are distinguished by different types of shutters and electronic circuitry.

a) The Flux Meter System

The integrating vertical anemometer can be used in combination with a cup anemometer to obtain the flux of momentum, according to the Reynolds formulation. The cup anemometer measures the wind's horizontal momentum. Simultaneously, the vertical motion of the air is determined at the same level by the integrating vertical anemometer. The two sensors are linked together electrically in this flux meter system so that the horizontal momentum of each ascending and descending layer is registered. The ascending units are added and the descending units are subtracted. The result is the total momentum flux. The eddy flux is obtained by subtracting the mass transport due to the mean motion,

$$\tau_z = -\overline{\rho w'u'} = -\rho(\overline{wu} - \overline{w}\,\overline{u}) = -\rho\left[\frac{\Sigma d\uparrow u - \Sigma d\downarrow u}{\Sigma \Delta t}\right] + \rho\bar{u}\left[\frac{\Sigma d\uparrow - \Sigma d\downarrow}{\Sigma \Delta t}\right] \qquad (6)$$

where $d\uparrow$ and $d\downarrow$ = the vertical motion in individual up and down anemometer rotations respectively. The negative sign is required since the downward flux is positive by convention. The flux of any other element is obtained by using instrumentation to give the concentration of the element in each ascending and descending parcel of air. The flux meter equations for evaporation and convective heat are

$$E = \left[\frac{\Sigma d\uparrow \rho_w - \Sigma d\downarrow \rho_w}{\Sigma \Delta t}\right] - \overline{\rho_w}\left[\frac{\Sigma d\uparrow - \Sigma d\downarrow}{\Delta t}\right]$$

$$H = \rho C_p\left[\frac{\Sigma d\uparrow T - \Sigma d\downarrow T}{\Sigma \Delta t}\right] - \rho \overline{C_p T}\left[\frac{\Sigma d\uparrow - \Sigma d\downarrow}{\Sigma \Delta t}\right]$$

in which E is evaporation, H is eddy heat flux, ρ_w is the vapor density, or absolute humidity of the air, T is potential temperature, and C_p is the specific heat of the air at constant pressure (see Thornthwaite, 1961).

The flux meter approach utilizes observations taken at a single level only and is to be preferred for use on Argus Island for that reason. Since the method gives the desired eddy flux as the difference between the total flux and the flux due to the mean vertical motion we believe that it can work satisfactorily in disturbed air. The instrumentation and the method of operation were described in detail in a recent Technical Report (Thornthwaite, 1961). A few paragraphs from that report are quoted to describe the method of operation of the flux meters:

> "To appreciate what is meant by the downward flux of momentum it is necessary to remember that the ascending and descending bodies of air also have horizontal components of velocity. Since the winds aloft are usually stronger than those near the ground, the descending air is moving faster horizontally and has a greater momentum than the rising air. Thus, there is usually a net downward flux of momentum. The horizontal component of the wind is obtained by use of the fast response sensor consisting of a lightweight rotating cup assembly. At the same time the vertical motion of the air is determined at that level. The two sensors are linked together in such a way that the horizontal momentum of every rising and descending layer of air is registered. The ascending units are added and the descending units are subtracted; the result is the momentum flux.
>
> "This is accomplished by using two recorders in parallel, both continuously following every change in horizontal wind speed, but wired to the vertical anemometer to record only the momentum of the ascending air layers on one and of the descending air layers on the other. The vertical anemometer merely serves to switch the indications to the proper recorder during updrafts and downdrafts. It also controls the chart advance of the recorders; each turn of the vane in the up direction results in unit advance of the chart on the up recorder and each down turn advances the down recorder one unit. For a given time interval the areas under the curves of the two charts give an integrated value of the upward and downward transport of momentum.

"The device for measuring the flux of sensible heat operates in a similar manner. Two recorders record the temperature of the air in the ascending and descending layers, using a fast response thermocouple as a sensor. Knowing the specific heat of the air it is easy to determine the quantity of sensible heat transported upward and downward, by measuring the areas under the curves on the two charts. The measurement of the eddy flux of water vapor (evaporation) from any natural surface involves the precise measurement of the water vapor density (absolute humidity) at a single convenient level above the evaporating surface by means of a fast response sensor, and simultaneously the measurement of the vertical motion of the air at that level. The humidity is measured by means of an automatic electronic dew point hygrometer while the vertical component of the wind is obtained by the vertical anemometer.

"The measurement of the flux of any element can be accomplished through the use of special sensors for the determination of the element in question. In all cases the combination of the vertical velocity anemometer with a suitable sensor to measure the element under investigation allows the direct measurement of the flux of the element. For example, the flux of ozone downward to the soil surface or the flux of radon or carbon dioxide upward from the soil could be determined. Complicated formulas and theories are avoided. It is simply a matter of measuring the concentration of the element in the air and the amount of air that moves upward and downward through a plane at that level where the sensors are mounted. The difference between these two measurements is the desired value." (pp. 7, 8)

A brief example from a previous study of turbulent conditions near the earth's surface which we carried out on a Signal Corps contract is included below to illustrate the type of results which are possible with the use of such instrumentation. In this example horizontal and vertical anemometers to provide the necessary information for the direct solution of equations for momentum flux were exposed at a height of 32 meters above a snow covered surface which was dotted with many roughness elements (trees, buildings, etc.) to a height of 12 to 15 meters. The day chosen, January 25, 1961, was associated with a strong outbreak of continental arctic air. The gradient flow over southern New Jersey was about 355°, and about 20 m sec^{-1}, giving surface winds of 5-7 m sec^{-1} during the day with an unstable stratification near the ground, and a surface wind direction of about 300°.

Two strip charts giving respectively $\Sigma d\uparrow u$ and $\Sigma d\downarrow u$ constitute the readout of the flux meter system. The two terms $\Sigma d\uparrow$ and $\Sigma d\downarrow$, respectively the sum of the up and down vertical run of the wind, are directly proportional to

the advance of the two strip charts. The terms $\Sigma u\uparrow$ and $\Sigma u\downarrow$, the horizontal velocity associated with each unit of up and down moving air are read and summed from the two strip charts. Knowing the sample time and air density, the total flux is then given by

$$\rho \left[\frac{\Sigma d\uparrow u - \Sigma d\downarrow u}{\Sigma \Delta t} \right]$$

After determining the mean flux according to the last term in equation 6, the eddy flux is simply the algebraic difference of the total and mean flux terms. This calculation is illustrated in table 2.

Table 2

Vertical Winds and Momentum Flux, 32 Meters
January 25, 1961

Hour Ending	Run of the Vertical Wind (meters)		Horizontal Velocity Average ($m\ sec^{-1}$)			Momentum Flux ($dynes\ cm^{-2}$)			Drag Coefficient*
	$\Sigma d\downarrow$	$\Sigma d\uparrow$	$\bar{u}\downarrow$	$\bar{u}\uparrow$	$\bar{u}$	Total	Mean	τ	C_D
1100	1093	1733	6.79	5.29	5.87	-6.30	-13.49	7.19	.016
1200	1175	1835	7.00	5.51	6.09	-6.79	-14.44	7.65	.016
1300	1053	1375	6.38	5.02	5.61	-0.68	- 6.50	5.82	.014
1400	783	1425	4.74	3.73	4.33	-5.77	- 9.99	4.22	.017
1500	883	1405	6.52	4.91	5.53	-4.12	-10.38	6.26	.016
1600	753	1463	6.55	5.15	5.63	-9.34	-14.36	5.02	.012
1700	715	909	4.80	3.57	4.09	-0.34	- 4.04	3.70	.017
1800	308	568	2.56	1.97	2.18	-1.19	- 2.04	0.85	.014

It will be noted that for this particular period and surface wind azimuth there was a strong preponderance of upflow - a reflection of the obstacles in the mean streamline, i.e., of standing waves related to the larger roughness elements. Hence there was a net upward momentum flux. In magnitude, however, this flux was much smaller than might have been expected, because the Reynolds term, or eddy flux, was directed strongly downwards. The horizontal wind speeds associated with updrafts and downdrafts are given in the table and show that the horizontal wind is much stronger in the downdrafts. Averages are given for convenience.

The eddy momentum flux, or Reynolds stress at 32 meters, has also been included in table 2. Values vary from 7.65 dynes cm^{-2} at 1200 hr, a very high value, to less than 1 dyne at 1800 hr. These figures may be compared with Lettau's estimate (1950) of 5.3 dynes cm^{-2} at Leipzig with a geostrophic wind of 17.5 m sec^{-1}.

* For definition, see following page.

The stress is, of course, a sensitive function of the wind speed, the static stability (partly because of the latter's influence on wind speed) and the surface wind azimuth. The values computed in the present case for the midday hours are typical of strong winds at neutral to moderately unstable stratification. The rapid decrease of wind speed and eddy stress after 1600 hr represented, in this case, the influence of increased stability and decreased gradient wind.

Direct measurement of the shearing stress is of immediate interest in studying the formation of ocean waves. The surface shearing stress represents the resistance offered by the ground or sea surface to the wind flow. Over land surfaces the stress in the layer for the first several meters above the surface is usually taken to equal the surface stress. There is conjecture that, in connection with wave formation, the stress over water may change with height. Simultaneous stress measurements at two levels over the ocean are therefore of immediate interest.

The drag of a surface is related to the wind velocity through a proportionality factor called the skin friction or surface drag coefficient C_D which is defined in the relation

$$\tau_o = C_D \rho \bar{u}_z^2$$

where τ_o is the surface shearing stress and u_z the velocity at a fixed height. Under neutral conditions the drag coefficient has been found constant for varying wind speeds over surfaces of a given roughness when the surface is rigid with respect to changes in $\bar{u}$. Over water, however, changes in $\bar{u}$ affect the surface roughness through wave formation, which changes the drag coefficient. Interest in the mechanism of wave development then, focuses on changes in drag coefficient with wind speed and wave height. Table 2 and figure 7 also give values of C_D over land calculated from the 32 meter shearing stress.

Figure 7 shows the relation of the drag coefficient to shearing stress (Reynolds stress at 32 meter) and wind velocity, $\bar{u}_{32}$, for several consecutive hours during the January 25 period cited previously. The first observation begins with the hour ending at 1100. Horizontal wind and eddy momentum flux reached their highest values (6.1 m sec^{-1}, 7.65 dynes cm^{-2}) at 1200. During the afternoon both wind speed and shearing stress diminished, but in such a manner that the drag coefficient remained nearly constant at 0.016 to 0.017. The wind blew steadily from the northwest during the afternoon. During the night the wind velocity dropped to 1-2 m sec^{-1} and the shearing stress was below 0.5 dynes cm^{-2}.

Most formulations for the drag coefficient are inherited from the profile era in micrometeorology, when the surface value of the eddy stress, the surface drag, was computed from measured vertical gradients of the time-averaged winds. Now that the stress itself is capable of direct measurement, interest may be

DRAG COEFFICIENT AS RELATED TO SHEARING STRESS AND MEAN WIND VELOCITY, CENTERTON, N.J., JANUARY 25-26, 1961

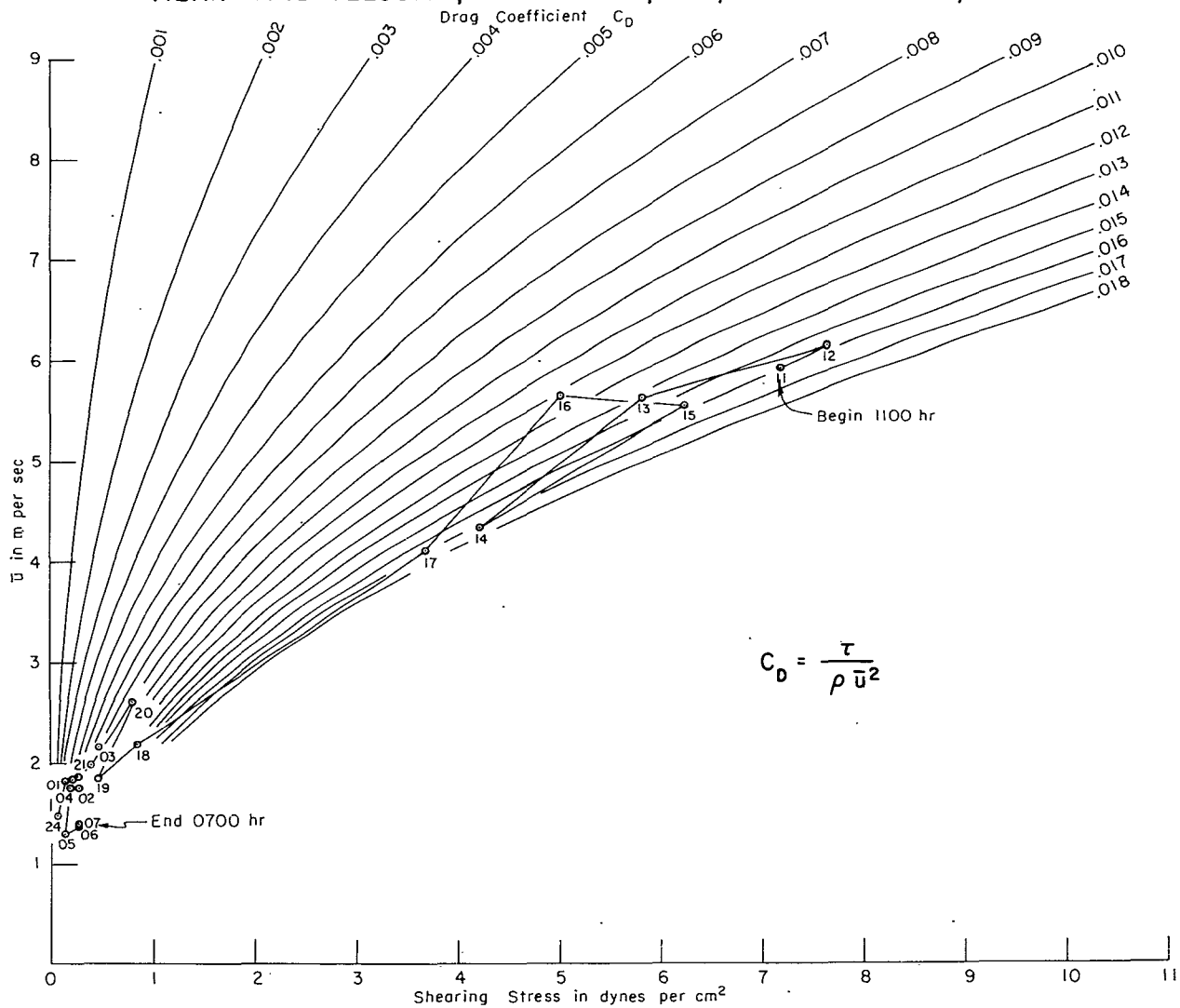

Figure 7

shifted to the control exerted by the gradient wind outside the boundary layer, since a major geophysical interest of the boundary layer is that it is the principal site of kinetic energy dissipation in the atmosphere; the surface drag, in other words, acts as a perpetual brake on the large-scale circulation in the free atmosphere. This has led Lettau (1959) to propose a geostrophic drag coefficient C_L, defined as

$$C_L = \left(\frac{\tau_0}{\rho}\right)^{1/2} / V_{g,0}$$

where τ_0 is the Reynolds stress at the surface and $V_{g,0}$ is the speed of the computed surface geostrophic wind.

Lettau's innovation makes possible a direct estimate of the rate of energy dissipation in the boundary layer if the angle α between the surface wind and geostrophic wind and the stability of the air layer can both be estimated. The numerical results for one hour during the observations of January 25 referred to above are summarized in table 3.

Table 3

Surface Drag and Energy Dissipation, Centerton, N.J.
Based on 32-Meter Stress Measurements

Date (1961)	Time Hr. End. (EST)	Ri_{100}	u_{32} deg/m sec^{-1}	$V_{g,0}$ deg/m sec^{-1}	α deg.	C_L	τ_{32} dynes cm^{-2}	K.E. Dissipation watts m^{-2}
Jan. 25	1300	-0.21	300/5.6	355/20.0	55	.034	5.82	6.85

Ri_{100} = Richardson number for 40 to 160 cm layer; u_{32} = 32 meter wind; $V_{g,0}$ = surface gradient wind; α = angle between surface wind and isobars; τ_{32} = eddy stress at 32 meters; K.E. = kinetic energy of boundary layer.

b) The Diffusion Meter System

There is a difference in the measurement of fluctuations in the horizontal and vertical wind. Gusts and lulls speed up and slow down the horizontal wind and account for the positive and negative fluctuations, but the motion continues in the positive direction and the anemometer continues to rotate in the same direction. With updrafts and downdrafts there is a reversal in the direction of the vertical wind and a corresponding reversal in the rotation of the vertical anemometer. Each updraft and each downdraft represents a distance of travel upward or downward in a given time. Thus, with the integrating vertical anemometer incorporated into the vertical diffusion system, we can easily obtain the following:

$D\uparrow$	=	total vertical motion up	(cm)
$D\downarrow$	=	total vertical motion down	(cm)
t	=	total sample period	(sec)
$\overline{w}$	=	$\frac{D\uparrow - D\downarrow}{t}$ = the mean vertical velocity	(cm sec^{-1})
$+\overline{w}$	=	$\frac{D\uparrow}{t}$ = the mean updraft velocity	(cm sec^{-1})
$-\overline{w}$	=	$\frac{D\downarrow}{t}$ = the mean downdraft velocity	(cm sec^{-1})

If the mean vertical wind is zero during the sample period, t, all velocity measurements will, by definition, be mean vertical eddy velocities, since

$$w' = w - \overline{w}$$

then

$$\overline{|w'|} = \frac{D\uparrow + D\downarrow}{t}$$

However, it has been noted above that the mean vertical wind over land surfaces seldom is zero even when averaged over periods as long as one hour. Consequently, it has been necessary to derive an expression for $\overline{|w'|}$ for practical use. Measurements under such conditions must, of necessity, be an approximation since the integrating anemometer is incapable of registering as velocity deviations from the mean those velocities which lie between zero and the mean velocity. For example, figure 8 represents a distribution of vertical velocities over a given time when the mean vertical velocity is not zero. The vertical anemometer is not capable of yielding as eddy velocities those velocities lying between zero and $\overline{w}$.

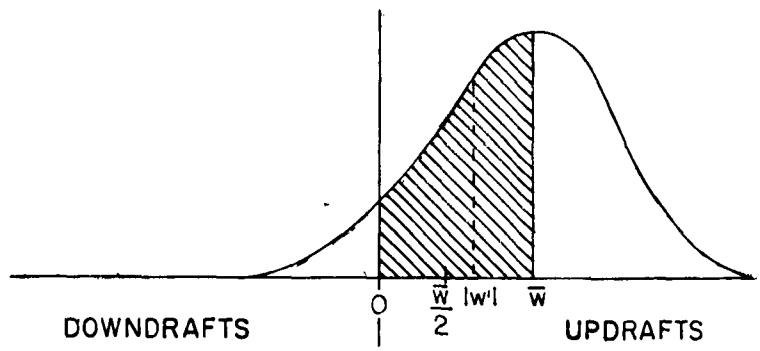

Figure 8

The expression, which was derived by Dr. A. K. Blackadar, and is given in Appendix I, assumes a Gaussian distribution of vertical velocities, a condition which is usually quite well fulfilled when the sample period is ten minutes or longer. The expression is

$$\overline{|w'|} = \left[\frac{D\uparrow + D\downarrow}{t} - \bar{w}\,\mathrm{erf}\left(\frac{\bar{w}}{\sigma_w}\right)\right] e^{\bar{w}^2/2\sigma_w^2}$$

which can be put in a form

$$\overline{|w'|} = a\,\frac{D\uparrow + D\downarrow}{t} \tag{7}$$

where a is a correction factor which may be expressed as a function of $D\uparrow/D\downarrow$. If $D\uparrow/D\downarrow$ lies in the interval $.5 \leq D\uparrow/D\downarrow \leq 2$, $\overline{|w'|}$ can be given by the simple expression above, omitting the correction factor, a, with an error of less than 4 percent. In open sites over land this condition is usually satisfied, and it is expected to be similarly fulfilled by observations taken at Argus Island.

The standard deviation of the vertical velocity is widely used in turbulence and diffusion studies. For Gaussian distributions the mean and standard deviation are directly related by the expression

$$\sigma_w = (\overline{w'^2})^{1/2} = \left(\frac{\pi}{2}\right)^{1/2} \overline{|w'|} \tag{8}$$

Recalling that the diffusion coefficient has the dimensions of velocity times a length, we may define empirical expression for K_m based on either the standard or mean deviations of the vertical velocity.

$$K_m = A\,z\,\overline{|w'|} \tag{9}$$

$$K_m = B\,z\,(\overline{w'^2})^{1/2}$$

where z, the height is taken as the appropriate order of magnitude for the eddy sizes, since near the ground they must be restricted by the surface. The coefficients A and B must be evaluated, but if the conditions of equation (8) are fulfilled, clearly $A = \sqrt{\pi/2}\,B$. Since these definitions are both strictly empirical, employing equation (9) has the advantage that $\overline{|w'|}$ is directly measured by the vertical anemometer.

The momentum, heat, and moisture fluxes would be given quite simply using a vertical diffusion meter together with a two cup anemometer, a two level temperature difference recording system, and humidity sensors at two levels. The expressions for momentum flux, τ, heat flux, H, and moisture flux, E, assuming $K_m = K_H = K_E$ are

$$\tau = -\rho K \frac{d\bar{u}}{dz}$$

$$H = \rho C_p K \frac{d\theta}{dz}$$

$$E = \rho K \frac{d\bar{q}}{dz}$$

Whether the three diffusion coefficients are equal should be made clear from simultaneous flux meter determinations.

Preliminary Flux Determinations

During the past year we have made a number of observations of momentum flux with our diffusion meter system to determine the turbulent exchange coefficient, K, from vertical wind measurements. The aim has been to increase our familiarity with the instrument's behavior under field conditions, to collect some data on the variation of vertical winds with height in the lowest few meters of the atmosphere, and to compare the results of momentum flux (shearing stress) measurements by several methods. The site for such studies should be a large, open level area of uniform surface roughness to insure measurement in an equilibrium turbulent wind field. Ideal sites are difficult to find near our Laboratory. The site where we obtained our observations during July and August, discussed below, was sufficiently level and extensive, allowing at least 1200 feet of unobstructed fetch. However, it was an agricultural field, planted in several sections to different crops. Although the surface roughness as determined by the measured profiles was always quite small, the roughness was different for winds from northern and southern sectors. Moreover, growing crops increased the roughness length from an initial low value of about .4 cm for a nearly bare field of sprouting beans to about 4 cm by August 14. More studies at this or better sites will be necessary to investigate the questions raised by these observations. The data collected so far have shown the need for changing the original approach, which was somewhat different from that of equation (9).

It was at first argued (Thornthwaite, 1962) that it would be possible to measure at a single point both the root mean square vertical velocity and a mean length of vertical displacement required by the definition of K_m in equation (5). The definition, interpretation, and measurement of the length l have long been the crux of the difficulty in turbulent diffusion studies. It is possible with the vertical anemometer to measure the number of updrafts and downdrafts during a given period. Since the mean vertical velocity is usually near zero, the number of updrafts and downdrafts will be a good estimate of the number of positive and negative vertical eddy displacements, thereby yielding the mean duration of these displacements. It was thought that the product of the mean eddy velocity and mean vertical displacement time would give the required length l. The number of updrafts and downdrafts is determined by counting the number of zero vertical

velocity crossings. The diffusion coefficient K_m would then be proportional to the expression

$$\sigma_w l = \sigma_w \frac{\overline{|w'|}\, t}{n} \qquad (10)$$

where n is the number of zero crossings in sample time t.

This expression was first tested in April 1962. The wind profile was measured at three levels, 40, 160, 320 cm and the vertical velocity measured at 260 cm. Momentum flux was calculated according to equations (1), (2), (3), and (10). The results, shown in figure 9, encouraged a more rigorous observational test which was undertaken in July and August.

The selected test site was the field described above. Anemometers for the profile were erected at 6 levels between .5 and 8 meters, and vertical wind anemometers placed at 4, 6, and 8 meters. Shearing stress calculated from the two profile equations (2) and (4) did not show uniformly good agreement. Stresses calculated by equation (10) for the three levels were neither consistent within themselves nor with the profile stresses. Lacking any theoretical basis for equation (10), it was therefore abandoned. The April results are especially fortuitous, since the vertical anemometer was mounted too close to the ground to record more than 80 percent of the vertical wind fluctuations.

It was necessary to return to the old assumption that the mixing length l, is proportional to the height, (equation (9)). Figures 10-12 show the shearing stresses determined on three occasions from the July-August series. During the run of July 26-27 the air was stable until about 0600. Throughout the run thereafter, near neutral conditions prevailed and the wind shear was nearly constant with height. Shearing stresses calculated from equation (9) (with A = .4) at both 6 and 8 meters for the whole run were in good agreement with each other and with the stress from Panofsky's wind profile, equation (4). The stress according to Kao's expression, equation (2), is not in good agreement with the others due, in part at least, to irregularities in the wind profile resulting from changing surface roughness with varying wind direction. As has been noted, Kao's expression is highly sensitive to profile irregularities.

Figure 11 shows the results of another run with the same equipment and at the same site, under somewhat unstable conditions during the afternoon of August 11. Apparently equation (9) for the 6 meter level with a value of A = .4 gives good agreement with Panofsky's and fair agreement with Kao's expressions. However the stresses calculated from the 8 meter vertical wind are only 60 percent of those calculated from the 6 meter level. Figure 12, for August 14, shows data from even more unstable conditions. Kao's and Panofsky's expressions are in fair agreement. For equation (9), however, A must be increased to about .5 to get agreement at the 6 meter level. Again the 8 meter level yielded stresses too low. Apparently, the factor A may be identified with von Karman's constant

under neutral and somewhat stable conditions, and under these conditions l is proportional to z. However, under unstable conditions the behavior of A is less clear. Apparently it must increase with instability, implying larger values of l (which is to be expected). However the implication is also that A must increase more rapidly then the height under unstable conditions, since, apparently, the vertical wind did not increase with height sufficiently to overcome the decreasing wind shear. The results of these observations strongly suggest that the diffusion coefficient for momentum can be directly obtained from vertical wind measurements when the air is adiabatic. Considerable further work will be required to extend the technique to diabatic conditions.

PROPOSED STUDY OF CLIMATIC FLUXES OVER THE SEA SURFACE

The present study, performed under a contract with the U. S. Naval Oceanographic Office, leads us to the conclusion that it will be possible to instrument the Argus Island platform so as to obtain reliable observations of various climatic fluxes over the sea surface without need for the installation of elaborate engineering structures to mount and expose instruments or for the construction of a separate Wand. At the present time it does not appear feasible to obtain systematic observations of climatic fluxes during all seasons of the year from any type of structure over the open sea in the Bermuda area. Hurricanes in the fall and severe winter storms limit the usefulness of the tower itself during the period from mid-September until about April. During these times it would make no difference whether the flux instrumentation was exposed on the tower or on separate structures near the tower. The high winds and waves, the salt spray, the vibration of the structures themselves, the variable direction of the winds, and the need to evacuate personnel as a safety precaution would all argue against the feasibility at present of an observation program through the late fall and winter months. Thus, we would propose that any program to determine the course of climatic fluxes over the sea surface at Argus Island be confined at first to the period from April 1 through September 30. At the present time, the expense and effort involved in operating during the remaining six months of the year, with no guaranty of any significant results, do not seem to be warranted. The experience of personnel on the platform during October and November of this year confirms the wisdom of this recommendation.

The pattern of airflow around the platform shown in figure 1 and the observations which were taken during the summer and fall of 1962 with winds from various directions indicate that measurements of the air properties must be made directly upwind of the structure to hold interference to a minimum.Therefore, we recommend that the instruments that must avoid the interference pattern be mounted permanently on the side that will give the best upwind exposure during the suggested April-September period of operation. Present indication is that the wind

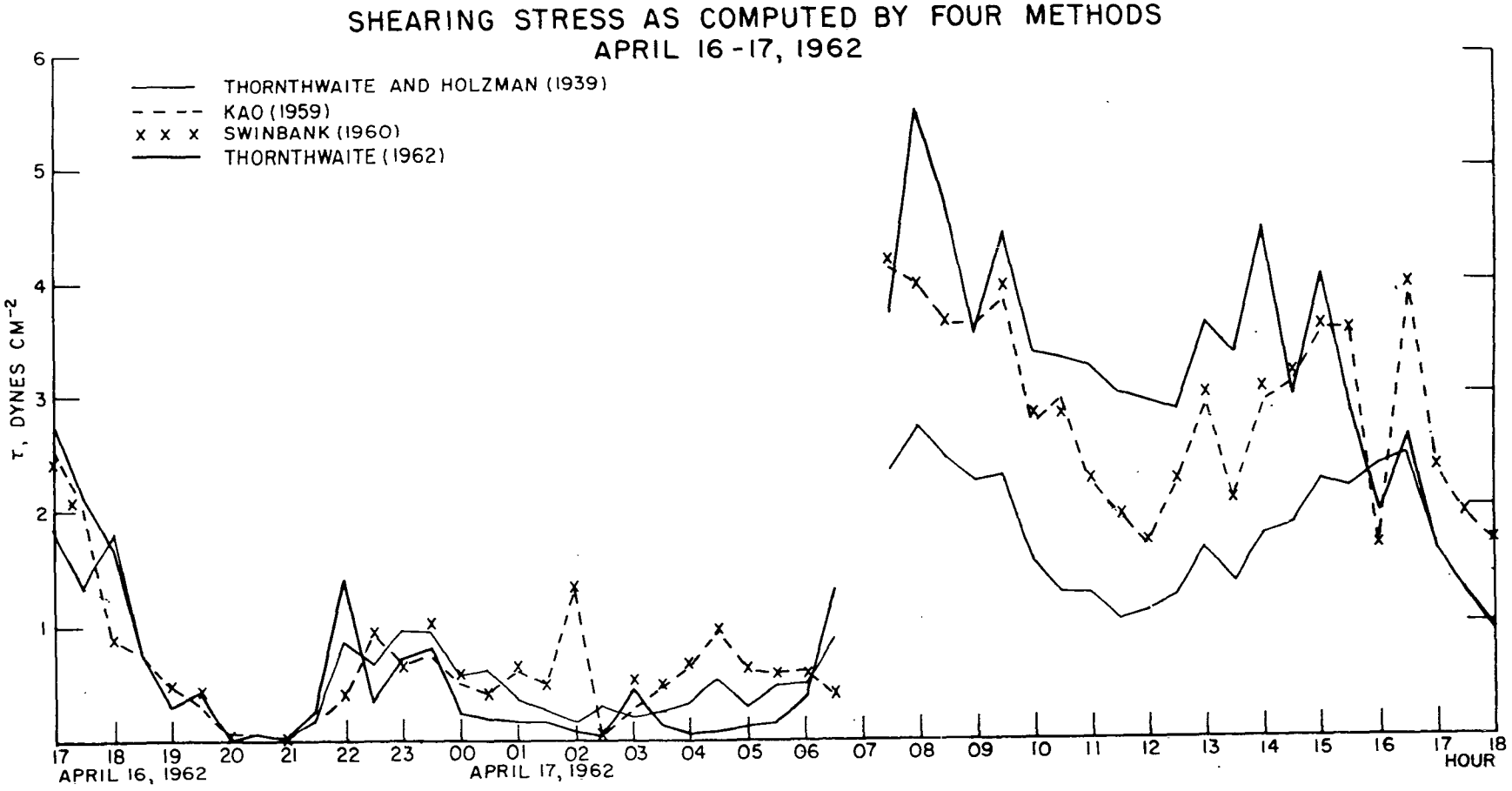
SHEARING STRESS AS COMPUTED BY FOUR METHODS
APRIL 16-17, 1962
THORNTHWAITE AND HOLZMAN (1939)
KAO (1959)
SWINBANK (1960)
THORNTHWAITE (1962)
τ, DYNES CM⁻²
6
5
4
3
2
1
17 18 19 20 21 22 23 00 01 02 03 04 05 06 07 08 09 10 11 12 13 14 15 16 17 18
HOUR
APRIL 16, 1962
APRIL 17, 1962

Figure 9

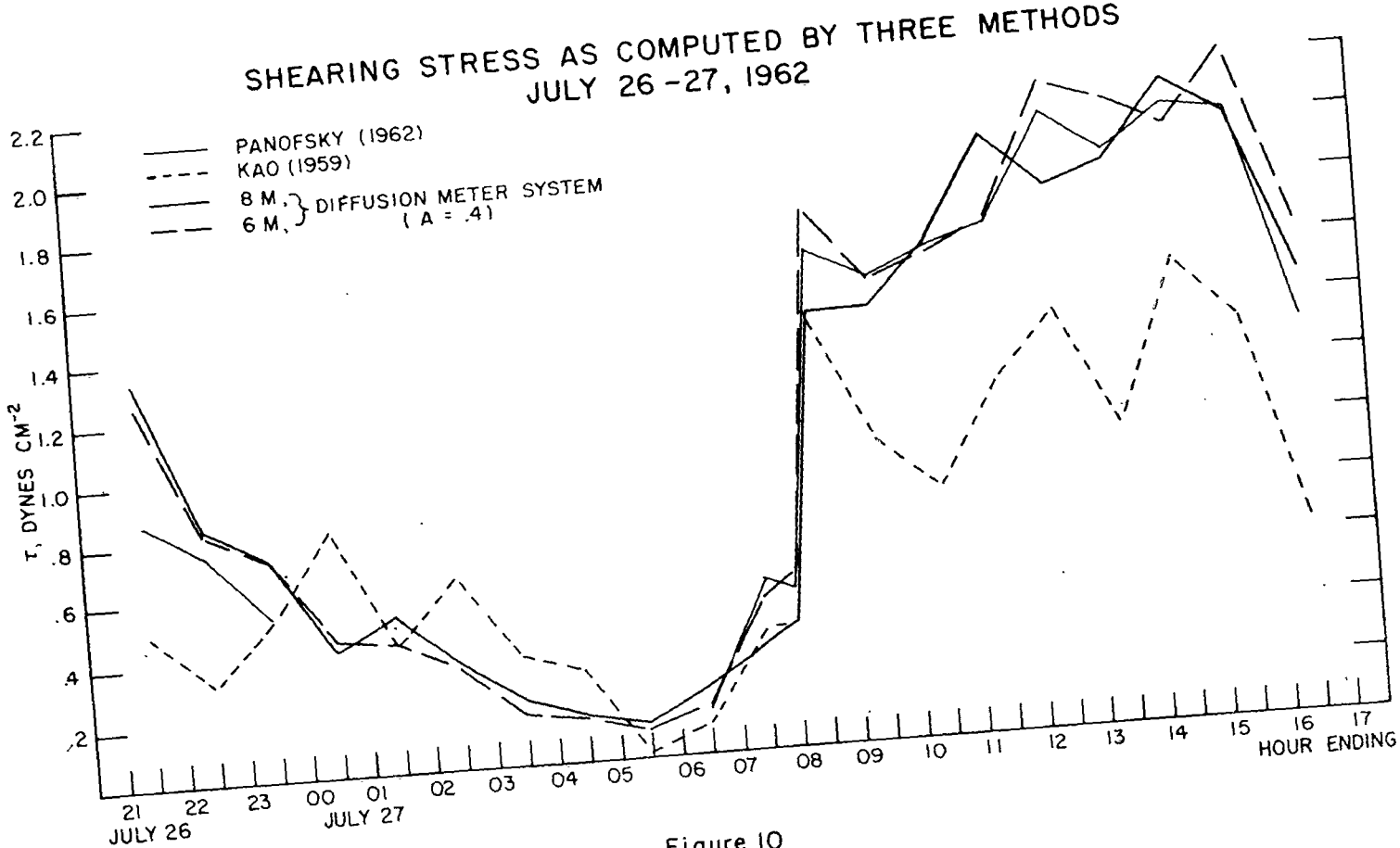
SHEARING STRESS AS COMPUTED BY THREE METHODS
JULY 26 -27, 1962
PANOFSKY (1962)
KAO (1959)
8 M.
6 M.
DIFFUSION METER SYSTEM
(A = .4)
τ, DYNES CM⁻²
2.2
2.0
1.8
1.6
1.4
1.2
1.0
.8
.6
.4
.2
21
22
23
00
01
02
03
04
05
06
07
08
09
10
11
12
13
14
15
16
17
HOUR ENDING
JULY 26
JULY 27

Figure 10

SHEARING STRESS AS COMPUTED BY THREE METHODS

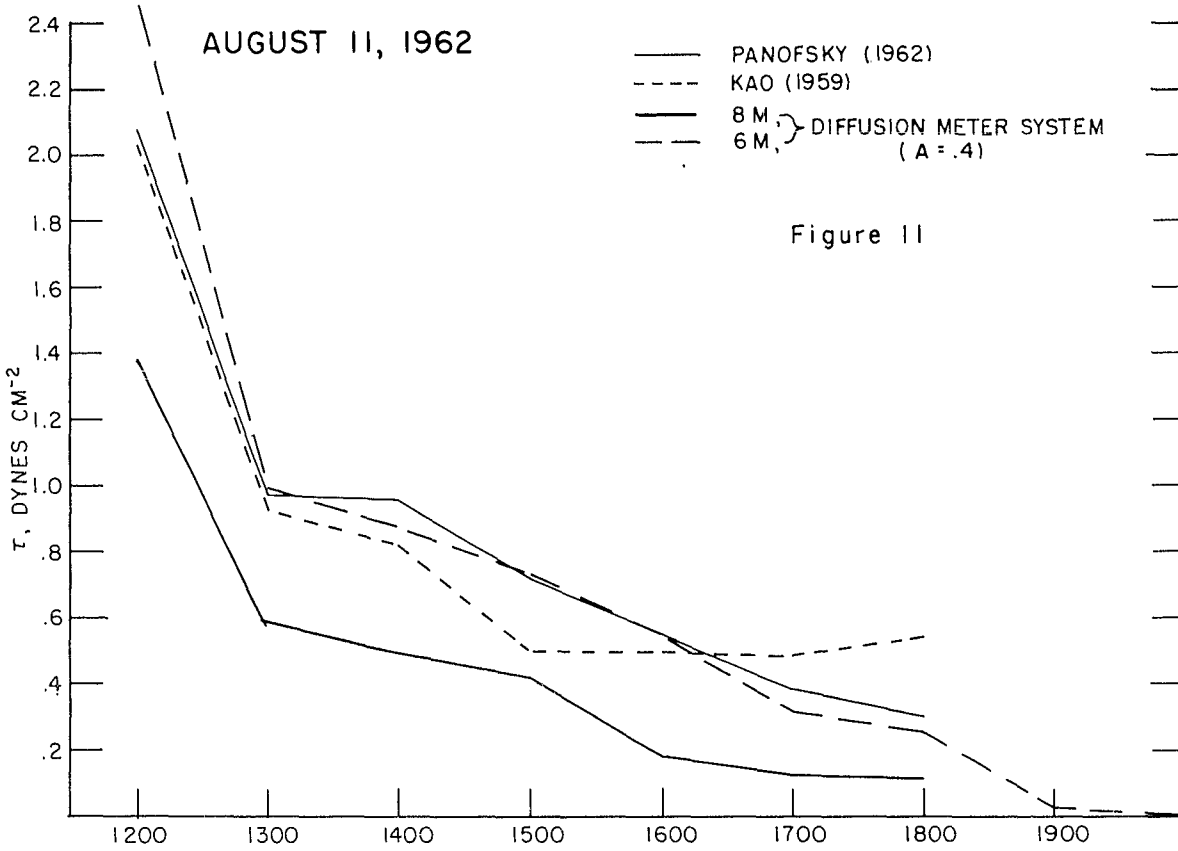

Figure 11

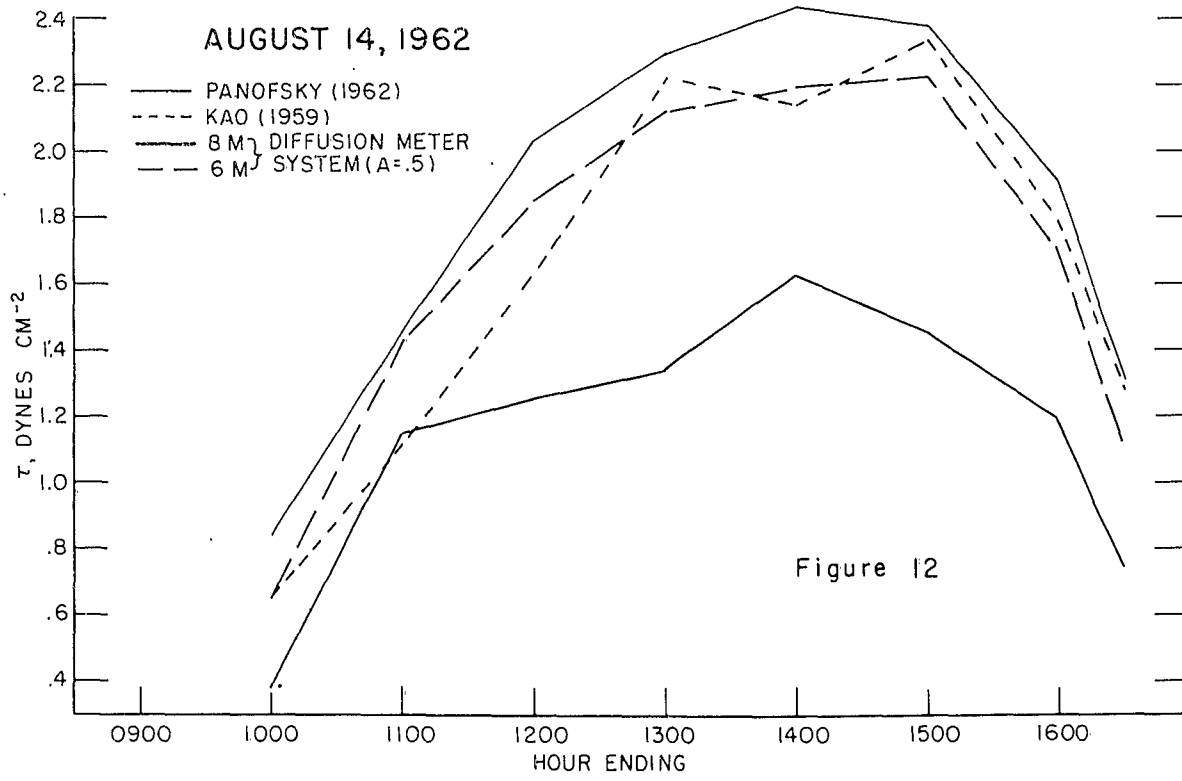

Figure 12

is from the south or southwest more than 50 percent of the time during these months. Figure 13 shows the percentage occurrence of wind direction at Argus Island by months for the one year period September 1961-August 1962. June, July, and August each showed a striking preference for south and southwest winds. During September the predominant wind shifted to the southeast, but 45 percent of all winds were still southerly. The wind during the rest of the autumn, winter and spring months were generally more evenly distributed about the points of the compass, or showed a preference for northerly directions. Consequently, the southern face of the platform is climatologically the most attractive location.

We recommend that a systematic program of flux measurements be undertaken, together with continuous recording of wind direction. It is possible that the platform itself could be calibrated to permit the flux observations made during times of unfavorable wind direction to be corrected. If such calibration is not feasible only the observations made under favorable conditions would be used; operation could be suspended at other times. While this would limit the periods of operations, it should provide sufficient observations to give the desired information on the course of climatic fluxes over the sea surface for a part of the year.

Analysis of the flow around Argus Island shows that the wind is disturbed for a considerable distance in all directions. Above and below the tower, or downwind from it there would appear to be no place for the exposure of instruments to avoid the influence of the platform itself. Forty to fifty feet out from the center of the windward face the vertical wind gradient is still affected by the disturbance of the platform. However, above the level of the platform and below it, the wind is not significantly disturbed to within forty feet of the platform. Thus, any system of flux determinations that involve making observations at only one level, or at the most two levels, could readily be installed and could be expected to operate without difficulty and give reliable results. Any system that requires accurate wind speeds at several levels would necessitate that the sensors be mounted at least sixty feet from the face of the platform. To get the sensors out that far would be difficult except through use of engineering structures that would be self-defeating. Accordingly, we favor use of the new methods of flux determination which do not depend on accurate wind profiles for obtaining the coefficient of turbulent diffusion.

The flux meter system requires just four sensors for the measurement of the fluxes of momentum, sensible heat and latent heat of evaporation: a sensitive cup anemometer, a vertical velocity anemometer, a temperature measuring device and an automatic dewpoint hygrometer. They are all mounted together at one fixed level. Since they must operate together, it is necessary that they all be matched as to speed of response. Otherwise, a certain part of the eddy flux being measured would be lost. We have succeeded in getting high and equal speeds of response from the horizontal and vertical anemometers and the temperature measuring system, and have made extensive series of observations of momentum flux and heat flux. Unfortunately, the automatic dewpoint hygrometer does not yet

have a sufficiently rapid speed of response to match the vertical anemometer, and thus the moisture flux system is not yet satisfactory. Further instrument development will be required before evaporation can be measured in this way.

The diffusion meter approach involves the use of a vertical anemometer to obtain the coefficient of turbulent diffusion, K, from observations at a single level. It requires, in addition, measurement of the property under investigation at two levels. The proportionality factor, A, involved in the definition of K would have to be determined for given heights and atmospheric conditions from comparison with the flux meter determinations. But, such comparisons of the two methods should add considerably to our knowledge of the utility of the simple diffusion meter system and the behavior under different conditions of the two factors, $\overline{|w'|}$ and $l = Az$.

The present fashion in data reduction is to attempt to record all data directly on tapes or punched cards for later analysis by machine methods. The meteorological sensors that we recommend for use on Argus Island are compatible with these systems, so it would be possible to adopt an elaborate data recording system. However, we would not recommend the setting up of such a system of data recording. Such electronic recording and processing systems are elaborate and costly and subject to breakdown. More time is often spent in getting the recording apparatus to function properly than in taking data. Such trouble on an isolated spot like Argus Island could result in the loss of many good days of observations when they are already limited by wind and weather conditions.

We have found that committing meteorologic data directly to tape or punch cards often results in the collection of data with little value. The data are not evaluated immediately and often malfunctions of the instruments cannot be spotted without a detailed study of the results. Thus, it is possible to collect long periods of worthless data. Then, also if the data are being reviewed by someone who has not had a hand in the collection of the data, it is often possible to miss some significant aspects. We would recommend therefore that the program of data collection be one that results in the ready availability of the data in a form for rapid evaluation and study. The collection system should be simple and relatively free from possible breakdown. In this connection we would recommend a system like our own Digital Printout Recorder which provides instant, legible and permanent reproductions of fixed interval data readings. The printout recorder uses the Polaroid® Land photographic process and thus offers immediate availability of the record. The meteorological information needed in this study could easily be made available in a form to be handled by the printout recorder. With printout of data occurring one per hour, the recorder will operate without attention for over two days. We have found this system of recording data on $3\frac{1}{4}$ by $4\frac{1}{4}$ cards to be extremely simple and entirely satisfactory for use both in the field and for later study in the office.

Polaroid® by Polaroid Corporation

SURFACE WIND DIRECTION, ARGUS ISLAND
1961 - 1962
PERCENTAGE FREQUENCY

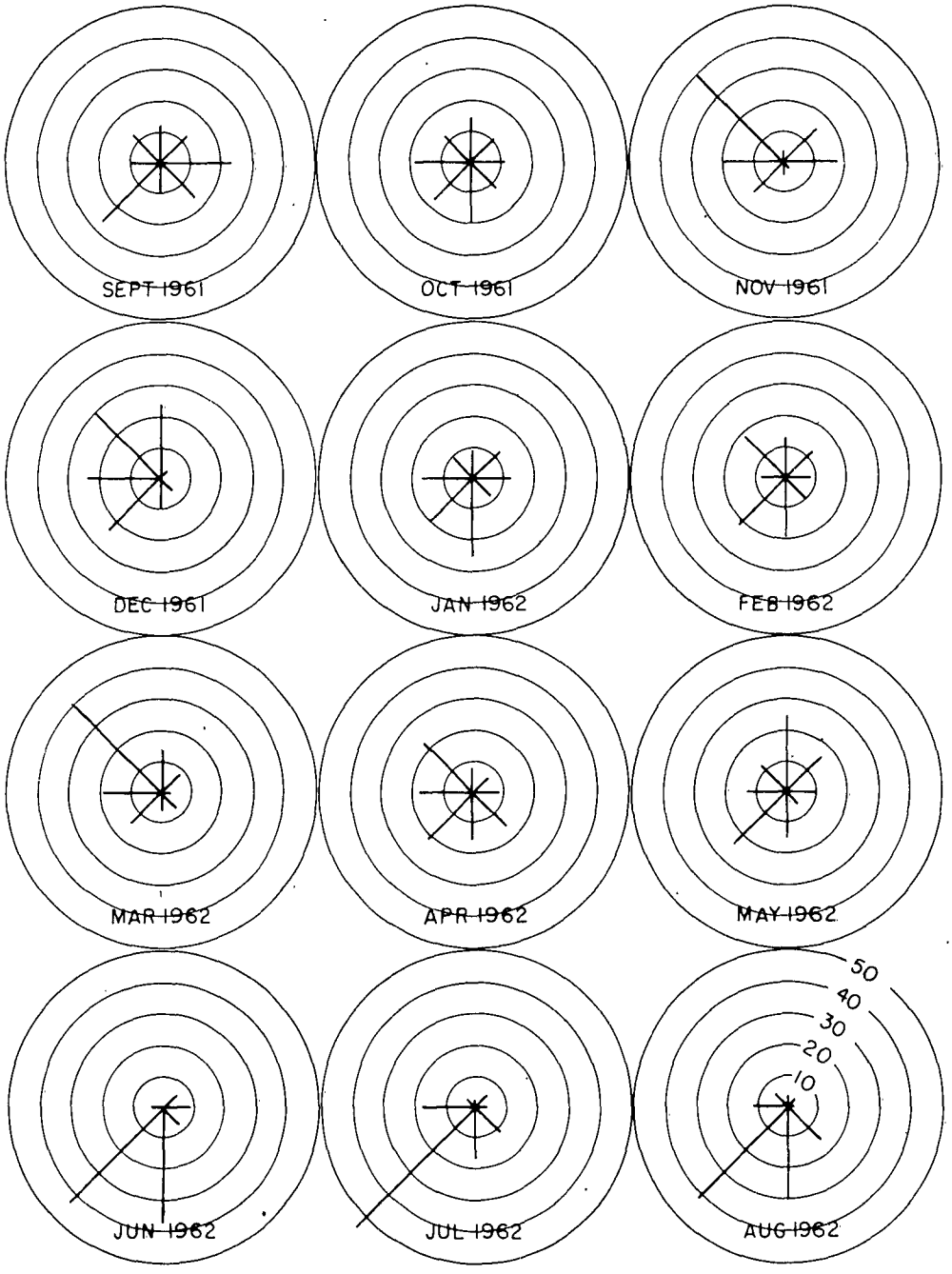

Figure 13

The taking of micrometeorological data is a very exacting task. In order to measure the small differences in meteorological parameters between adjacent locations, matched sensors which respond rapidly and accurately to even small changes or fluctuations in these parameters are needed. Such sensors must be lightweight and free from friction or inertia, and thus are often fairly delicate and fragile. They are not designed for routine operation, unattended for long periods of time. Those instruments which are so ruggedly constructed as to be able to withstand environmental conditions for weeks or months without attention are not satisfactory for the purposes of micrometeorological studies. Thus, it should become apparent that any micrometeorological study, whether on land or over the sea should only be undertaken when it is possible to provide regular service and care of the sensors themselves.

When it is recognized that micrometeorological research studies require continuous attention by trained and experienced personnel, it becomes clear that much of the present effort to develop telemetering systems for the remote and continuous recording of data will not yield significant results. The two programs are not compatible. In the micrometeorological study the need is for sensitive and responsive instruments which will of necessity require frequent attention and servicing while in the program for remote recording of data over a long time period on a routine basis, the need is for rugged instruments that will be fairly insensitive to environmental influence. It should be understood that there is a need for both types of studies, for the routine observations as well as for the detailed micrometeorological observations. But before beginning any meteorological program it should be determined which type of results are sought and then the type of instruments and recording systems which will give those results can be selected.

The experience which we have gained during the observation program of 1962 has given us a new insight into the problems of making reliable micrometeorological observations over a sea surface. Although it is beyond the scope of the present preliminary survey, we have become aware of the great difficulty in utilizing ships as observation platforms for climatic studies over the oceans. It is evident that shipboard observations made anywhere other than from the bow when the ship is heading into the wind would be greatly disturbed, and unreliable. A survey of the pattern of wind flow around a moving ship similar to the present study of the wind flow around Argus Island would be well worthwhile.

ACKNOWLEDGMENT

Several members of the staff joined in various phases of the present research study. The work was carried out under the general direction of Dr. C. W. Thornthwaite. Instrumentation and sensor mounting problems, and the actual site surveys on the tower were under the supervision of Mr. William Superior. The observation program was carried out by Ray Ono, Richard Field, and Wayne Rouse as well as by Mr. Superior during the course of three visits to the tower. Dr. Alfred K. Blackadar, of Pennsylvania State University, gave valuable assistance in the planning of the survey and in the development of the equations for use with the flux meters. Data analysis was principally carried out by Richard Field and Wayne Rouse. The present report was prepared by Dr. C. W. Thornthwaite, Dr. J. R. Mather, William Superior and Richard Field. Drafting was by Katsuma Nishimoto. The report was typed by Mrs. Helen Bano. We wish to express our appreciation to other members of the staff of the Laboratory for their help in the completion of the present study. Thanks are also due to Dean Kenneth Hare of McGill University for reading the manuscript and for his help in preparing figure 7.

We would also like to express our appreciation to Mr. Robert B. Elder and Mr. Robert L. Pickett of the U. S. Naval Oceanographic Office for their assistance in the installation and operation of the instruments on Argus Island and for facilitating the transport of needed equipment to the site.

REFERENCES

Blackadar, A. K.
1959 "Study of Forecasting Low-Level Wind Gradients," Final Report, Contract AF19(604)-2059, Penn. State Univ., Dept. of Meteorology, 96 pp.

Brocks, K.
1959 "Ein Neues Gerät für Störungsfreie Meteorologische Messungen auf dem Meer," Archiv für Meteorologie, Geophysik, und Bioklimatologie, Serie A, Band 11, Heft 2, pp. 227-239.

Brunt, D.
1952 Physical and Dynamical Meteorology. Cambridge, Cambridge Univ. Press, 428 pp. (2nd Edition) (1st Edition, 1934)

Deacon, E. L.
1949 "Vertical Diffusion in the Lowest Layers of the Atmosphere," Quart. Jour. Royal Met. Soc., Vol. 75, pp. 89-103.

Sheppard, P. A., and Webb, E. K.
1956 "Wind Profiles over the Sea and the Drag at the Sea Surface," Aust. Journal of Physics, Vol. 9, No. 4, pp. 511-541.

Geiger, R.
1951 "Microclimatology," in Compendium of Meteorology, ed. by T. Malone, Boston, American Meteorology Society.

Halstead, M.
1943 "A Stability Term in the Wind-Gradient Equation," Trans. Amer. Geophys. U., Vol. 24, pp. 204-208.

Holzman, B.
1943 "The Influence of Stability on Evaporation," Annals New York Acad. Sci., Vol. XLIV, Art. 1, pp. 13-18.

Jacobs, W. C.
1942 "On the Energy Exchange between Sea and Atmosphere," Sears Foundation, Journal of Marine Research, Vol. V., No. 1, pp. 37-66.

Jones, J. I. P. and Pasquill, F.
1959 "An Experimental System for Directly Recording Statistics of the Intensity of Atmospheric Turbulence," Quart. Jour. Royal Met. Soc., Vol. 85, pp. 225-236.

Kao, S. K.
1959 "Turbulent Transfer in the Boundary Layer of a Stratified Fluid," Jour. Met., Vol. 16, No. 5, pp. 497-503.

Lettau, H. H.
1950 "A Re-examination of the 'Leipzig Wind Profile' Considering Some Relations between Wind and Turbulence in the Frictional Layer," Tellus, Vol. 2, pp. 125-129.

1957 "Windprofil, Innere Reibung, und Energieumsatz in den unteren 500 m uber dem Meer," Beitr zur Phys. der Atmos., Vol. 30, pp. 78-96.

1959 "Wind Profile, Surface Stress and Geostrophic Drag Coefficients in the Atmospheric Surface Layer," p. 243 in Advances in Geophysics, Vol. 6, Academic Press, New York.

Montgomery, R. B.
1940 "Observations of Vertical Humidity Distribution above the Ocean Surface and Relation to Evaporation," Papers in Phys. Ocean. Meteor., Mass. Inst. Tech. and Woods Hole Ocean. Inst., Vol. III, No. 4, 30 pp.

Panofsky, H. A.
1962 "Determination of Stress from Wind and Temperature Measurements," (unpublished).

Blackadar, A.K., and McVehil, G.E.
1960 "The Diabatic Wind Profile," Quart. Jour. Royal Met. Soc., Vol. 86, pp. 390-398.

Pasquill, F.
1962 Atmospheric Diffusion. London, D. van Nostrand, 297 pp.

Priestley, C. H. B.
1959 Turbulent Transfer in the Lower Atmosphere. Chicago, Univ. of Chicago Press, 130 pp.

Roll, H. U.
1948 "Das Windfeld über den Meereswellen," Die Naturwissenschaften, Jahr. 35, Heft 8, pp. 230-234.

1948a "Wassernahes Windprofil und Wellen auf dem Wattenmeer," Annalen der Meteorologie, April-May, pp. 139-151.

Roll, H. U. (continued)

1949 "Vergleichende Betrachtung und Kritik von Windprofilmessungen auf See," Annalen der Meteorologie, March-April, pp. 71-78.

1951 "Neue Messungen zur Entstehung von Wasserwellen durch Wind," Annalen der Meteorologie, Heft 1-6, pp. 269-286.

Rossby, C. G.

1932 "A Generalization of the Theory of the Mixing Length with Applications to Atmospheric and Oceanic Turbulence," Mass. Inst. Tech., Met. Papers, 1(4): 36 pp.

1936 "On the Frictional Force between Air and Water and on the Occurrence of a Laminar Boundary Layer Next to the Surface of the Sea," Papers in Phys. Ocean. Meteor., Mass. Inst. Tech., Woods Hole Ocean. Inst., Vol. 4, No. 3, I.

and Montgomery, R. B.

1935 "The Layer of Frictional Influence in Wind and Ocean Currents," Papers in Phys. Ocean. Meteor., Mass. Inst. Tech., Woods Hole Ocean. Inst., Vol. 3, No. 3, 101 pp.

Sutton, O. G.

1932 "A Theory of Eddy Diffusion in the Atmosphere," Proc. Roy. Soc., (A), Vol. 135, pp. 143-165.

1934 "Wind Structure and Evaporation in a Turbulent Atmosphere," Proc. Roy. Soc. London, A, Vol. 146, pp. 701-722.

1953 Micrometeorology. New York, McGraw Hill.

Sverdrup, H. U.

1937 "On the Evaporation from the Oceans," Sears Foundation, Journal of Marine Research, Vol. 1, No. 1, pp. 3-14.

1940 "On the Annual and Diurnal Variation of the Evaporation from the Oceans," Sears Foundation, Journal of Marine Research, Vol. III, No. 2, pp. 93-104.

Swinbank, W. C.

1960 "Wind Profile in Thermally Stratified Flow," Nature, Vol. 186, No. 4732, pp. 463-464.

Taylor, G. I.

1921 "Diffusion by Continuous Movements," Proc. London Math. Soc., Ser. 2, Vol. 20, p. 196.

Thornthwaite, C. W.
1961 "The Measurement of Climatic Fluxes," Tech. Report No. 1, Contract Nonr 2997(00), Laboratory of Climatology, 19 pp.

1962 "Development of an Ozone Flux Meter," Final Report, Contract Cwb 10097, Laboratory of Climatology, 14 pp.

and Holzman, B.
1939 "The Determination of Evaporation from Land and Water Surfaces," Monthly Weather Rev., 67, pp. 4-11.

and Holzman, B.
1940 "A Year of Evaporation from a Natural Land Surface," Amer. Geophys. Union, Trans., 21, pp. 510-511.

and Holzman, B.
1942 "Measurement of Evaporation from Land and Water Surfaces," Tech. Bull. 817, U.S.D.A., Washington, 75 pp.

Superior, W. J., Mather, J. R. and Hare, F. K.
1961 "Measurement of Vertical Winds and Momentum Flux," Publications in Climatology, Laboratory of Climatology, Vol. XIV, No. 1, 89 pp.

APPENDIX I

EQUATION FOR DETERMINING $\overline{|w'|}$ BY MEANS OF THE INTEGRATING VERTICAL ANEMOMETER

by

A. K. Blackadar

We presume that observations of vertical velocity are integrated over a sufficiently long time that D represents the sum of a nearly infinite set of individual values of w. Heretofore, we have treated these as a serial set in time, but now we shall sort these according to values of w into classes at intervals dw, which we regard as infinitesimal. We define the probability function p(w) as

$$p(w) = \frac{dn}{N\,dw} \tag{1}$$

where dn is the number in the given class interval of width dw, and N is the total number in all classes. From the definition we have

$$\int_{-\infty}^{\infty} p(w)\,dw = 1 \tag{2}$$

We may presume that the values of w that determine the probability function are representative of equal time intervals. In this case dn/N is simply the fraction of the total time t when this velocity prevails. With this in mind it is easy to see that the mean velocity is given by

$$\bar{w} = \int_{-\infty}^{\infty} w\,p(w)\,dw \tag{3}$$

and the two travel distances by

$$\left.\begin{aligned} D\uparrow &= t\int_{0}^{\infty} w\,p(w)\,dw \\ D\downarrow &= -t\int_{-\infty}^{0} w\,p(w)\,dw \end{aligned}\right\} \tag{4}$$

The minus sign is required because D↓ is positive although the associated vertical velocities are negative. By combining (3) and (4) we obtain

$$\bar{w} = \frac{D\uparrow - D\downarrow}{t} \tag{5}$$

Now define w' in the usual way

$$w' = w - \bar{w} \tag{6}$$

The mean magnitude of w' can be computed by the equation

$$\overline{|w'|} = \int_{w'=0}^{\infty} w' \, p(w) \, dw - \int_{-\infty}^{w'=0} w' \, p(w) \, dw \tag{7}$$

the minus sign of the second term being required because over the range of integration $|w'| = -w'$. We wish to express $\overline{|w'|}$ in terms of $D\uparrow$ and $D\downarrow$, so we rewrite (7) in the form

$$\overline{|w'|} = \int_{\bar{w}}^{\infty} (w-\bar{w}) \, p(w) \, dw - \int_{-\infty}^{\bar{w}} (w-\bar{w}) \, p(w) \, dw \tag{8}$$

which can be transformed by regrouping the ranges of integration

$$\overline{|w'|} = \int_{0}^{\infty} (w-\bar{w}) \, p(w) \, dw - \int_{-\infty}^{0} (w-\bar{w}) \, p(w) \, dw - 2\int_{0}^{\bar{w}} (w-\bar{w}) \, p(w) \, dw \tag{9}$$

$$= \frac{D\uparrow + D\downarrow}{t} - \bar{w}\left[\int_{0}^{\infty} p(w) \, dw - \int_{-\infty}^{0} p(w) \, dw\right] - 2\int_{0}^{\bar{w}} (w-\bar{w}) \, p(w) \, dw$$

Now, $p(w)\,dw$ may be interpreted as the fraction of the total time that the velocity w prevails. By the further use of identities and the application of (2) we may get the form

$$\overline{|w'|} = \frac{D\uparrow + D\downarrow}{t} - \bar{w}\left(2\int_{\bar{w}}^{\infty} p(w) \, dw - 1\right) - 2\int_{0}^{\bar{w}} w \, p(w) \, dw \tag{10}$$

This is about as far as one can proceed without knowing the frequency distribution $p(w)$. In most cases experience has shown this to be normal, but with convective conditions at moderate levels the distribution becomes asymmetric - a few large upward velocities and a large number of smaller downward velocities.

In the case where a normal distribution prevails we have

$$p(w) = \frac{1}{\sigma\sqrt{2\pi}} e^{-w'^2/2\sigma^2} \tag{11}$$

with σ representing the standard deviation of w. From (7) we have

$$\overline{|w'|} = \frac{1}{\sigma}\sqrt{\frac{2}{\pi}}\int_0^\infty w' e^{-w'^2/2\sigma^2}\,dw = \sigma\sqrt{\frac{2}{\pi}} \tag{12}$$

$$\text{or} \quad \sigma = 1.25\,\overline{|w'|}$$

For the terms in (10) we find

$$2\int_{\bar{w}}^\infty p(w)\,dw - 1 = \frac{2}{\sigma\sqrt{2\pi}}\int_0^\infty e^{-w'^2/2\sigma^2}\,dw' - 1 = 0$$

$$\int_0^{\bar{w}} wp(w)\,dw = \frac{\bar{w}}{\sigma\sqrt{2\pi}}\int_0^{\bar{w}} e^{-w'^2/2\sigma^2}\,dw' + \frac{1}{\sigma\sqrt{2\pi}}\int_{-\bar{w}}^0 w' e^{-w'^2/2\sigma^2}\,dw' \tag{13}$$

$$= \frac{\bar{w}}{2}\,\mathrm{erf}\left(\frac{\bar{w}}{\sigma}\right) - \frac{\sigma}{\sqrt{2\pi}}\left(1 - e^{-\bar{w}^2/2\sigma^2}\right) \tag{14}$$

where $\mathrm{erf}(\bar{w}/\sigma)$ is the error function defined by the equation

$$\mathrm{erf}(x) = \sqrt{\frac{2}{\pi}}\int_0^x e^{-\theta^2/2}\,d\theta \tag{15}$$

It is the area under the normal curve of unit standard deviation between x and -x. From (10), (13), and (14) we get

$$\overline{|w'|} = \frac{D\uparrow + D\downarrow}{t} + \sqrt{\frac{2}{\pi}}\,\sigma - \sqrt{\frac{2}{\pi}}\,\sigma e^{-\bar{w}^2/2\sigma^2} - \bar{w}\,\mathrm{erf}\left(\frac{\bar{w}}{\sigma}\right) \tag{16}$$

This can be simplified by using (12) as follows

$$\overline{|w'|} = \left[\frac{D\uparrow + D\downarrow}{t} - \bar{w}\,\mathrm{erf}\left(\frac{\bar{w}}{\sigma}\right)\right] e^{\bar{w}^2/2\sigma} \tag{17}$$

This can be put in a form

$$\overline{|w'|} = a\left(\frac{D\uparrow + D\downarrow}{t}\right)$$

$$\text{or} \qquad a = \frac{\overline{|w'|}\, t}{D\downarrow + D\uparrow} \tag{18}$$

in which the coefficient a is a function of $\bar{w}/\overline{|w'|}$ or if desired, a function of $D\uparrow/D\downarrow$. Calculation of a and $\overline{|w'|}/\bar{w}$ as functions of $D\uparrow/D\downarrow$ are presented in table 4 using (17), (12), and (5), and a graph displaying the results is shown in figure 14.

From figure 14 we see that if $D\uparrow/D\downarrow$ is anywhere between 0.5 and 2.0, we can determine $\overline{|w'|}$ from the following simple formula

$$\overline{|w|} = \frac{D\uparrow + D\downarrow}{t}$$

with less than 4 percent error.

The situation for large values of $D\uparrow/D\downarrow$ is more difficult to assess, as it appears possible that a does not approach any limit as $D\uparrow/D\downarrow \longrightarrow \infty$ (i.e., as $D\downarrow \longrightarrow 0$). Instead, it may continue to decrease without approaching zero. At any rate, sooner or later $D\downarrow$ becomes so small that its value is actually unknown (fractional turns of the vane do not register) and really large values of $D\uparrow/D\downarrow$ become indeterminable. The graph shows this may happen even through $\overline{|w'|}$ is still a substantial fraction of $\bar{w}$. A simple calculation shows, for example, that if $\bar{w}$ were four times as large as $\overline{|w'|}$, $D\downarrow$ is only one hundredth of one percent as large as $D\uparrow$.

THE COEFFICIENT a AS A FUNCTION OF THE RATIO OF UPDRAFTS TO DOWNDRAFTS

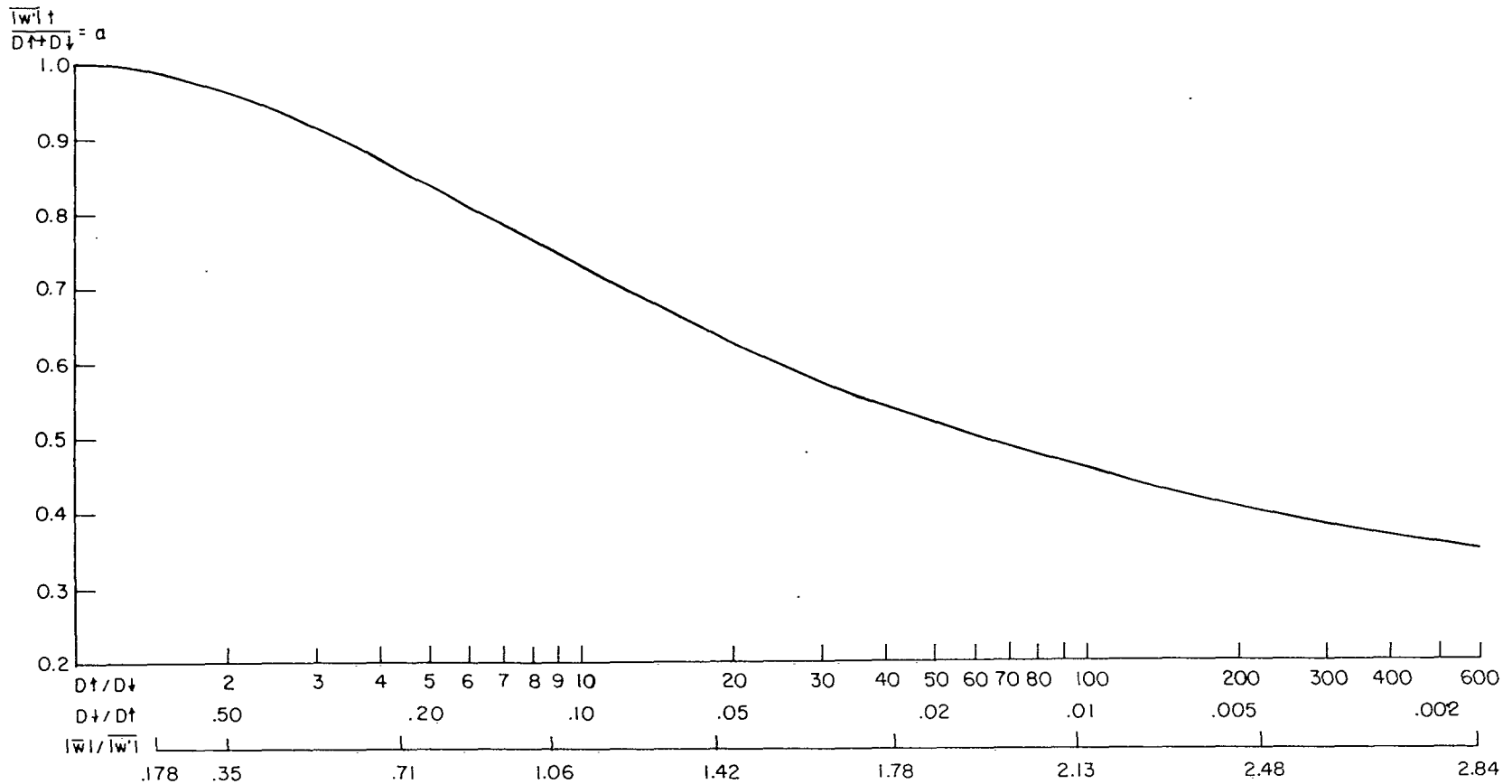

Figure 14

Table 4

Calculations for the Coefficient a

θ^*	θ^2	$\bar{w}/\overline{\lvert w'\rvert}$	e^{θ^2}	$\frac{\overline{\lvert w'\rvert}}{\bar{w}} e^{-\bar{w}^2/2\sigma^2}$	$\operatorname{erf}(\frac{\bar{w}}{\sigma})$	$\frac{D\uparrow+D\downarrow}{D\uparrow-D\downarrow}$ **	a ***	$D\uparrow/D\downarrow$ $\bar{w}>0$	$D\uparrow/D\downarrow$ $\bar{w}<0$
.00	.0000	.0000	1.0000	∞	.0000	∞	1.000	1.00	1.000
.02	.0004	.0354	1.0004	28.237	.0225	28.259	1.000	1.07	.932
.05	.0025	.0886	1.0025	11.258	.0564	11.314	.997	1.19	.838
.08	.0064	.1418	1.0064	7.007	.0900	7.097	.994	1.33	.753
.10	.0100	.1772	1.0100	5.588	.1124	5.700	.990	1.43	.701
.12	.0144	.2126	1.0145	4.636	.1347	4.771	.986	1.53	.653
.14	.0196	.2481	1.0198	3.952	.1569	4.109	.981	1.64	.608
.16	.0256	.2835	1.0259	3.438	.1790	3.617	.975	1.73	.567
.18	.0324	.3188	1.0329	3.037	.2009	3.238	.969	1.89	.528
.20	.0400	.3544	1.0408	2.711	.2227	2.934	.962	2.04	.491
.22	.0484	.3898	1.0496	2.444	.2443	2.688	.954	2.18	.458
.24	.0576	.4253	1.0593	2.220	.2732	2.493	.943	2.34	.427
.26	.0676	.4607	1.0699	2.029	.2869	2.316	.937	2.52	.397
.28	.0786	.4962	1.0818	1.863	.3079	2.171	.928	2.71	.369
.30	.0900	.5316	1.0942	1.719	.3287	2.048	.918	2.91	.344
.32	.1024	.5670	1.1078	1.592	.3491	1.941	.909	3.13	.320
.34	.1156	.6025	1.1225	1.479	.3693	1.848	.898	3.35	.298
.36	.1296	.6369	1.1384	1.377	.3893	1.766	.888	3.61	.277
.40	.1600	.7088	1.1735	1.202	.4280	1.630	.866	4.18	.239
.60	.360	1.064	1.433	0.6557	.6036	1.2593	.746	8.72	.1146
.80	.640	1.419	1.896	0.3716	.7416	1.1132	.634	18.5	.0540
1.00	1.000	1.775	2.718	0.2075	.8426	1.0501	.536	40.9	.0244
1.20	1.440	2.130	4.221	0.1112	.9100	1.0212	.460	95.4	.0105
1.40	1.960	2.483	7.099	0.0567	.9524	1.0091	.399	221.	.0045
1.60	2.560	2.840	12.94	0.0272	.9762	1.0034	.351	590.	.0017
1.80	3.240	3.195	25.53	0.0123	.9890	1.0013	.315	1,540.	.0006
2.00	4.000	3.549	54.60	0.0052	.9954	1.0006	.282	3,340.	.0003
2.20	4.840	3.904	126.5	0.0020	.9982	1.0002	.256	10,000.	-
2.40	5.760	4.255	319.	0.0007	.9994	1.0001	.235	20,000.	-
2.60	6.760	4.610	860.	0.0003	.9998	1.0001	.217	-	-

* $\theta = \bar{w}/\sqrt{2}\,\sigma = \bar{w}/\sqrt{\pi}\,\overline{\lvert w'\rvert}$

** $\frac{D\uparrow+D\downarrow}{D\uparrow-D\downarrow} = \frac{D\uparrow+D\downarrow}{\bar{w}\,t} = \operatorname{erf}(\frac{\bar{w}}{\sigma}) + \frac{\overline{\lvert w'\rvert}}{\bar{w}} e^{-\bar{w}^2/2\sigma^2}$

*** $a = \lvert w'\rvert t/D\uparrow+D\downarrow = \frac{D\uparrow-D\downarrow}{D\uparrow+D\downarrow} \cdot \frac{\overline{\lvert w'\rvert}}{\bar{w}}$

APPENDIX II

Observed Wind Velocities and Velocity Ratios, Argus Island, August-October 1962

August 16, 1962

Run 1, 1850-1900 AST*, WD 180°

Position**	u_z***	u_z/u_T
Tower	479	
0, 116	564	1.177
0, 112	-	-
0, 108	506	1.056
0, 104	438	.914
0, 100	384	.802

Run 2, 1902-1912, WD 180°

Position	u_z	u_z/u_T
Tower	439	
0, 116	468	1.066
0, 112	429	.977
0, 108	335	.763
0, 104	227	.517
0, 100	200	.456

Run 3, 1615-1625, WD 180°

Position	u_z	u_z/u_T
Tower	443	
20, 116	505	1.140
20, 112	510	1.151
20, 108	478	1.079
20, 104	293	.661
20, 100	156	.352

Run 4, 1625-1635, WD 180°

Position	u_z	u_z/u_T
Tower	374	
20, 116	394	1.053
20, 112	405	1.083
20, 108	426	1.139
20, 104	340	.909
20, 100	177	.473

Run 5, 1635-1645, WD 180°

Position	u_z	u_z/u_T
Tower	280	
20, 116	292	1.043
20, 112	293	1.046
20, 108	310	1.107
20, 104	280	1.000
20, 100	180	.643

Run 6, 1646-1656, WD 180°

Position	u_z	u_z/u_T
Tower	482	
20, 116	530	1.100
20, 112	550	1.141
20, 108	571	1.185
20, 104	523	1.085
20. 100	384	.797

Run 7, 1821-1831, WD 180°

Position	u_z	u_z/u_T
Tower	437	
20, 116	501	1.146
20, 112	512	1.172
20, 108	398	.911
20, 104	187	.428
20, 100	129	.295

September 23, 1962

Run 8, 2115-2125, WD 186°

Position	u_z	u_z/u_T
Tower	1044	
43, 139	986	.944
43, 129	995	.953
43, 119	994	.952
43, 109	1040	.996
43, 101	1095	1.049

* All times are Atlantic Standard Time

** Position by Cartesian coordinates as in figure 1

*** All velocities in cm sec^{-1}

August 17, 1962

Run 9, 2125-2135, WD 186°

Position	u_z	u_z/u_T
Tower	1122	
43, 139	1048	.934
43, 129	1059	.944
43, 119	1053	.938
43, 109	1100	.980
43, 101	1163	1.036

Run 10, 2135-2145, WD 187°

Position	u_z	u_z/u_T
Tower	1008	
43, 139	961	.953
43, 129	969	.961
43, 119	972	.964
43, 109	1014	1.006
43, 101	1071	1.062

Run 11, 1302-1312, WD 180°

Position	u_z	u_z/u_T
Tower	506	
43, 116	467	.925
43, 112	470	.929
43, 108	488	.964
43, 104	502	.992
43, 100	486	.960

Run 12, 1314-1324, WD 180°

Position	u_z	u_z/u_T
Tower	506	
43, 116	476	.941
43, 112	488	.964
43, 108	503	.994
43, 104	519	1.026
43, 100	481	.951

Run 13, 1328-1338, WD 180°

Position	u_z	u_z/u_T
Tower	535	
43, 116	501	.936
43, 112	512	.957
43, 108	527	.985
43, 104	546	1.021
43, 100	511	.955

Run 14, 1339-1349, WD 180°

Position	u_z	u_z/u_T
Tower	531	
43, 116	498	.938
43, 112	510	.960
43, 108	524	.987
43, 104	544	1.024
43, 100	507	.955

Run 15, 1350-1400, WD 180°

Position	u_z	u_z/u_T
Tower	574	
43, 116	536	.934
43, 112	552	.962
43, 108	565	.984
43, 104	589	1.026
43, 100	541	.942

Run 16, 1406-1416, WD 180°

Position	u_z	u_z/u_T
Tower	558	
43, 116	526	.943
43, 112	540	.968
43, 108	557	.998
43, 104	581	1.041
43, 100	533	.955

October 24, 1962

Run 17, 0940-0950, WD 230°

Position	u_z	u_z/u_T
Tower	1030	
57, 136	926	.900
57, 116	901	.875
57, 100	776	.754
57, 87	628	.610
57, 80	600	.583
57, 73	641	.622

Run 18, 0950-1000, WD 230°

Position	u_z	u_z/u_T
Tower	982	
57, 136	917	.934
57, 116	860	.876
57, 100	738	.752
57, 87	582	.593
57, 80	555	.565
57, 73	603	.614

Run 19, 1006-1016, WD 225°

Position	u_z	u_z/u_T
Tower	935	
57, 136	875	.936
57, 116	819	.875
57, 100	700	.748
57, 87	545	.583
57, 80	518	.554
57, 73	568	.607

September 24, 1962

Run 20, 0840-0850, WD 197°

Position	u_z	u_z/u_T
Tower	814	
111, 99	686	.842
101, 99	651	.800
91, 99	627	.770
81, 99	735	.903
61, 99	710	.872
41, 99	689	.846

Run 21, 0850-0900, WD 203°

Position	u_z	u_z/u_T
Tower	880	
111, 99	733	.832
101, 99	688	.781
91, 99	675	.767
81, 99	788	.896
61, 99	774	.879
41, 99	762	.865

Run 22, 0900-0910, WD 203°

Position	u_z	u_z/u_T
Tower	938	
111, 99	780	.832
101, 99	735	.784
91, 99	720	.768
81, 99	840	.896
61, 99	826	.881
41, 99	812	.866

Run 23, 1155-1205, WD 182°

Position	u_z	u_z/u_T
Tower	550	
75, 95	473	.860
67, 95	458	.832
57, 95	436	.792
47, 95	406	.738
45, 95	409	.744

Run 24, 1205-1215, WD 182°

Position	u_z	u_z/u_T
Tower	1080	
75, 95	920	.851
67, 95	890	.824
57, 95	863	.799
47, 95	790	.731
45, 95	794	.735

Run 25, 1215-1225, WD 178°

Position	u_z	u_z/u_T
Tower	688	
75, 95	592	.861
67, 95	577	.838
57, 95	557	.809
47, 95	520	.756
45, 95	524	.762

October 26, 1962

Run 26, 1530-1540, WD 280°

Position	u_z	u_z/u_T
Tower	928	
99, 20	782	.843
89, 20	-	-
79, 20	-	-
69, 20	792	.854
59, 20	806	.869

Run 27, 1545-1555, WD 270°

Position	u_z	u_z/u_T
Tower	875	
99, 20	725	.829
89, 20	-	-
79, 20	-	-
69, 20	726	.830
59, 20	754	.862

Run 28, 1600-1610, WD 270°

Position	u_z	u_z/u_T
Tower	772	
99, 20	684	.884
89, 20	-	-
79, 20	-	-
69, 20	675	.874
59, 20	711	.919

Run 29, 1650-1700, WD 275°

Position	u_z	u_z/u_T
Tower	818	
99, 20	662	.809
89, 20	-	-
79, 20	-	-
69, 20	646	.789
59, 20	706	.864

Run 30, 1715-1725, WD 275°

Position	u_z	u_z/u_T
Tower	858	
99, 20	706	.824
89, 20	-	-
79, 20	-	-
69, 20	728	.848
59, 20	742	.866

Run 31, 1805-1815, WD 270°

Position	u_z	u_z/u_T
Tower	717	
99, 20	637	.889
89, 20	644	.898
79, 20	-	-
69, 20	649	.906
59, 20	661	.922

Run 32, 2300-2310, WD 260°

Position	u_z	u_z/u_T
Tower	782	
99, 20	645	.825
89, 20	650	.831
79, 20	-	-
69, 20	654	.836
59, 20	662	.846

Run 33, 2320-2330, WD 260°

Position	u_z	u_z/u_T
Tower	782	
99, 20	643	.822
89, 20	-	-
79, 20	-	-
69, 20	648	.828
59, 20	660	.844

October 23, 1962

Run 34, 1736-1746, WD 205°

Position	u_z	u_z/u_T
Tower	876	
76, 82	650	.742
76, 62	674	.769
76, 45	704	.804
76, 33	714	.815
76, 23	694	.793
76, 17	654	.747

Run 35, 1747-1757, WD 210°

Position	u_z	u_z/u_T
Tower	852	
76, 82	637	.748
76, 62	657	.771
76, 45	679	.797
76, 33	686	.806
76, 23	667	.783
76, 17	629	.739

Run 36, 1758-1808, WD 210°

Position	u_z	u_z/u_T
Tower	792	
76, 82	580	.733
76, 62	605	.764
76, 45	627	.791
76, 33	634	.801
76, 23	618	.780
76, 17	582	.735

Run 37, 1810-1820, WD 210°

Position	u_z	u_z/u_T
Tower	815	
76, 82	610	.748
76, 62	632	.775
76, 45	655	.803
76, 33	664	.815
76, 23	648	.795
76, 17	612	.751

Run 38, 1820-1830, WD 210°

Position	u_z	u_z/u_T
Tower	858	
76, 82	636	.741
76, 62	658	.766
76, 45	683	.796
76, 33	688	.801
76, 23	665	.775
76, 17	628	.731

Run 39, 1830-1840, WD 210°

Position	u_z	u_z/u_T
Tower	902	
76, 82	673	.746
76, 62	695	.771
76, 45	719	.798
76, 33	720	.799
76, 23	696	.772
76, 17	655	.726

Run 40, 1840-1850, WD 205°

Position	u_z	u_z/u_T
Tower	867	
76, 82	643	.742
76, 62	665	.767
76, 45	693	.799
76, 33	698	.805
76, 23	676	.779
76, 17	635	.732

Run 41, 1613-1623, WD 220°

Position	u_z	u_z/u_T
Tower	853	
66, 82	583	.684
66, 62	623	.731
66, 45	679	.796
66, 33	694	.814
66, 23	674	.790
66, 17	636	.746

Run 42, 1624-1634, WD 220°

Position	u_z	u_z/u_T
Tower	882	
66, 82	601	.681
66, 62	641	.727
66, 45	697	.790
66, 33	717	.812
66, 23	694	.787
66, 17	654	.741

Run 43, 1635-1645, WD 220°

Position	u_z	u_z/u_T
Tower	863	
66, 82	593	.687
66, 62	631	.731
66, 45	684	.793
66, 33	698	.809
66, 23	679	.787
66, 17	640	.742

Run 44, 1645-1655, WD 210°

Position	u_z	u_z/u_T
Tower	850	
66, 82	582	.684
66, 62	622	.732
66, 45	700	.823
66, 33	690	.812
66, 23	670	.788
66, 17	636	.748

Run 45, 1355-1405, WD 225°

Position	u_z	u_z/u_T
Tower	704	
57, 82	414	.589
57, 62	518	.736
57, 45	572	.813
57, 33	574	.815
57, 23	565	.802
57, 17	532	.756

Run 46, 1407-1417, WD 225°

Position	u_z	u_z/u_T
Tower	737	
57, 82	438	.594
57, 62	546	.740
57, 45	604	.819
57, 33	605	.820
57, 23	589	.799
57, 17	551	.748

Run 47, 1419-1429, WD 225°

Position	u_z	u_z/u_T
Tower	753	
57, 82	451	.599
57, 62	559	.743
57, 45	622	.826
57, 33	627	.833
57, 23	614	.816
57, 17	579	.769

Run 48, 1430-1440, WD 227°

Position	u_z	u_z/u_T
Tower	759	
57, 82	432	.569
57, 62	559	.737
57, 45	622	.820
57, 33	626	.825
57, 23	609	.802
57, 17	571	.753

October 24, 1962

Run 49, 0845-0855, WD 220°

Position	u_z	u_z/u_T
Tower	1082	
57, 78	548	.507
57, 58	807	.746
57, 41	852	.788
57, 28	855	.791
57, 19	820	.758
57, 12	746	.690

Run 50, 0900-0910, WD 225°

Position	u_z	u_z/u_T
Tower	1091	
57, 78	555	.509
57, 58	811	.744
57, 41	860	.788
57, 28	864	.792
57, 19	827	.758
57, 12	750	.688

Run 51, 0910-0920, WD 225°

Position	u_z	u_z/u_T
Tower	1060	
57, 78	563	.531
57, 58	799	.753
57, 41	837	.790
57, 28	834	.787
57, 19	808	.762
57, 12	724	.683

September 27-28, 1962

Run 52, 2309-2319, WD 190°

Position	u_z	u_z/u_T
Tower	1030	
52, 64	882	.856
52, 47	924	.898
52, 37	950	.922
52, 27	936	.909
52, 17	875	.849

Run 53, 2322-2329, WD 184°

Position	u_z	u_z/u_T
Tower	1071	
52, 64	849	.793
52, 47	886	.828
52, 37	901	.841
52, 27	875	.817
52, 17	818	.764

Run 54, 2330-2400, WD 180°

Position	u_z	u_z/u_T
Tower	1081	
52, 64	934	.864
52, 47	957	.885
52, 37	964	.892
52, 27	948	.877
52, 17	886	.819

Run 55, 0001-0031, WD 184°

Position	u_z	u_z/u_T
Tower	1115	
52, 64	947	.849
52, 47	978	.877
52, 37	994	.891
52, 27	975	.874
52, 17	912	.817

Run 56, 0032-0102, WD 182°

Position	u_z	u_z/u_T
Tower	1141	
52, 64	996	.872
52, 47	1024	.898
52, 37	1037	.901
52, 27	1015	.889
52, 17	950	.832

Run 57, 0430-0455, WD 187°

Position	u_z	u_z/uT
Tower	1038	
52, 64	853	.822
52, 47	888	.856
52, 37	904	.871
52, 27	890	.857
52, 17	831	.800

Run 58, 0500-0525, WD 205°

Position	u_z	u_z/uT
Tower	987	
52, 64	818	.829
52, 47	839	.851
52, 37	878	.890
52, 27	859	.871
52, 17	819	.830

Run 59, 0530-0555, WD 203°

Position	u_z	u_z/uT
Tower	918	
52, 64	727	.792
52, 47	807	.878
52, 37	796	.867
52, 27	779	.849
52, 17	736	.801

Run 60, 0600-0625, WD 197°

Position	u_z	u_z/uT
Tower	978	
52, 64	805	.823
52, 47	852	.871
52, 37	874	.893
52, 27	861	.880
52, 17	808	.826

Run 61, 0630-0655, WD 197°

Position	u_z	u_z/uT
Tower	849	
52, 64	710	.835
52, 47	752	.886
52, 37	769	.905
52, 27	762	.898
52, 17	720	.847

Run 62, 0655-0730, WD 192°

Position	u_z	u_z/uT
Tower	855	
52, 64	705	.825
52, 47	748	.875
52, 37	764	.894
52, 27	753	.881
52, 17	703	.823

Run 63, 0730-0755, WD 185°

Position	u_z	u_z/uT
Tower	815	
52, 64	688	.844
52, 47	728	.892
52, 37	736	.903
52, 27	728	.894
52, 17	677	.830

August 17-18, 1962

Run 64, 2130-2140, WD 180°

Position	u_z	u_z/uT
Tower	380	
52, 69	182	.479
52, 65	266	.700
52, 61	285	.750
52, 57	292	.768
52, 53	293	.771

Run 65, 2141-2151, WD 180°

Position	u_z	u_z/u_T
Tower	390	
52, 69	188	.482
52, 65	272	.697
52, 61	292	.749
52, 57	304	.779
52, 53	306	.785

Run 66, 2152-2202, WD 180°

Position	u_z	u_z/u_T
Tower	453	
52, 69	219	.483
52, 65	317	.700
52, 61	340	.751
52, 57	353	.779
52, 53	354	.781

Run 67, 2203-2213, WD 180°

Position	u_z	u_z/u_T
Tower	451	
52, 69	219	.486
52, 65	322	.714
52, 61	345	.765
52, 57	358	.794
52, 53	360	.798

Run 68, 2214-2224, WD 180°

Position	u_z	u_z/u_T
Tower	460	
52, 69	229	.498
52, 65	330	.717
52, 61	352	.765
52, 57	364	.791
52, 53	365	.793

Run 69, 2224-2234, WD 180°

Position	u_z	u_z/u_T
Tower	386	
52, 69	189	.490
52, 65	278	.720
52, 61	299	.775
52, 57	308	.798
52, 53	311	.806

Run 70, 0845-0855, WD 180°

Position	u_z	u_z/u_T
Tower	593	
52, 69	312	.526
52, 65	429	.723
52, 61	455	.767
52, 57	474	.799
52, 53	475	.801

September 18, 1962

Run 71, 1345-1355, WD 237°

Position	u_z	u_z/u_T
Tower	840	
30, 67	365	.435
30, 57	785	.935
30, 47	751	.894
30, 37	738	.879

Run 72, 1355-1405, WD 232°

Position	u_z	u_z/u_T
Tower	718	
30, 67	304	.423
30, 57	698	.971
30, 47	642	.893
30, 37	641	.892

September 17-18, 1962

Run 73, 1406-1416, WD 230°

Position	u_z	u_z/u_T
Tower	761	
30, 67	328	.430
30, 57	702	.922
30, 47	657	.863
30, 37	642	.843

Run 74, 1245-1255, WD 225°

Position	u_z	u_z/u_T
Tower	893	
26, 57	888	.989
27, 47	-	-
28, 37	799	.895
29, 27	765	.856

Run 75, 1255-1305, WD 225°

Position	u_z	u_z/u_T
Tower	904	
26, 57	897	.992
27, 47	831	.919
28, 37	805	.890
29, 27	767	.848

Run 76, 1305-1315, WD 247°

Position	u_z	u_z/u_T
Tower	904	
26, 57	890	.984
27, 47	816	.903
28, 37	786	.869
29, 27	750	.830

Run 77, 1315-1325, WD 237°

Position	u_z	u_z/u_T
Tower	846	
26, 57	844	.998
27, 47	781	.923
28, 37	764	.903
29, 27	728	.860

Run 78, 2145-2155, WD 180°

Position	u_z	u_z/u_T
Tower	909	
27, 47	890	.979
28, 37	822	.904
29, 27	760	.836
30, 17	736	.810

Run 79, 2200-2210, WD 180°

Position	u_z	u_z/u_T
Tower	957	
27, 47	982	1.026
28, 37	904	.945
29, 27	831	.868
30, 17	793	.829

Run 80, 2210-2220, WD 180°

Position	u_z	u_z/u_T
Tower	908	
27, 47	918	1.011
28, 37	852	.938
29, 27	788	.868
30, 17	754	.830

Run 81, 0920-0930, WD 203°

Position	u_z	u_z/u_T
Tower	768	
27, 47	759	.988
28, 37	697	.908
29, 27	599	.780
30, 17	618	.805

Run 82, 0930-0940, WD 203°

Position	u_z	u_z/u_T
Tower	884	
27, 47	868	.982
28, 37	798	.903
29, 27	708	.801
30, 17	708	.801

Run 83, 0945-0955, WD 225°

Position	u_z	u_z/u_T
Tower	970	
27, 47	944	.974
28, 37	862	.889
29, 27	788	.812
30, 17	702	.724

Run 84, 1000-1010, WD 225°

Position	u_z	u_z/u_T
Tower	976	
27, 47	948	.971
28, 37	871	.892
29, 27	792	.811
30, 17	792	.811

Run 85, 1010-1020, WD 225°

Position	u_z	u_z/u_T
Tower	924	
27, 47	880	.952
28, 37	810	.876
29, 27	747	.808
30, 17	723	.782

Run 86, 1550-1600, WD 233°

Position	u_z	u_z/u_T
Tower	796	
17, 68	410	.514
17, 60	802	1.007
17, 50	747	.938
17, 40	702	.881

Run 87, 1600-1610, WD 236°

Position	u_z	u_z/u_T
Tower	728	
17, 68	371	.510
17, 60	759	1.043
17, 50	716	.984
17, 40	665	.913

Run 88, 1610-1620, WD 238°

Position	u_z	u_z/u_T
Tower	785	
17, 68	422	.538
17, 60	782	.996
17, 50	729	.929
17, 40	675	.860

September 19, 1962

Run 89, 1710-1720, WD 275°

Position	u_z	u_z/u_T
Tower	618	
-10, 53	-	-
-10, 43	522	.844
-10, 33	539	.873
-10, 23	506	.819

Run 90, 1720-1730, WD 275°

Position	u_z	u_z/u_T
Tower	589	
-10, 53	436	.739
-10, 43	487	.826
-10, 33	496	.842
-10, 23	453	.769

Run 91, 1730-1740, WD 274°

Position	u_z	u_z/u_T
Tower	533	
-10, 53	381	.715
-10, 43	441	.827
-10, 33	456	.856
-10, 23	436	.818

Run 92, 1615-1625, WD 261°

Position	u_z	u_z/u_T
Tower	477	
-10, 63	388	.813
-10, 53	390	.818
-10, 43	290	.608
-10, 33	400	.839

Run 93, 1625-1635, WD 268°

Position	u_z	u_z/u_T
Tower	479	
-10, 63	362	.756
-10, 53	364	.760
-10, 43	310	.647
-10, 33	461	.962

Run 94, 1635-1645, WD 274°

Position	u_z	u_z/u_T
Tower	448	
-10, 63	417	.931
-10, 53	386	.862
-10, 43	380	.848
-10, 33	439	.980

Run 95, 1530-1540, WD 262°

Position	u_z	u_z/u_T
Tower	512	
-10, 68	353	.689
-10, 58	396	.773
-10, 48	366	.715
-10, 38	454	.887

Run 96, 1540-1550, WD 264°

Position	u_z	u_z/u_T
Tower	450	
-10, 68	341	.758
-10, 58	389	.864
-10, 48	320	.711
-10, 38	460	1.022

Run 97, 1550-1600, WD 266°

Position	u_z	u_z/u_T
Tower	398	
-10, 68	299	.751
-10, 58	414	1.040
-10, 48	278	.698
-10, 38	426	1.070

Run 98, 1415-1425, WD 242°

Position	u_z	u_z/u_T
Tower	498	
-18, 70	432	.867
-18, 60	481	.966
-18, 50	474	.952
-18, 40	445	.894

Run 99, 1425-1435, WD 244°

Position	u_z	u_z/u_T
Tower	463	
-18, 70	425	.918
-18, 60	450	.972
-18, 50	444	.959
-18, 40	442	.955

Run 100, 1435-1445, WD 246°

Position	u_z	u_z/u_T
Tower	525	
-18, 70	470	.895
-18, 60	504	.960
-18, 50	503	.958
-18, 40	500	.952

Run 101, 1100-1110, WD 288°

Position	u_z	u_z/u_T
Tower	552	
-18, 45	469	.850
-18, 35	482	.873
-18, 25	453	.821
-18, 15	396	.717

Run 102, 1110-1120, WD 285°

Position	u_z	u_z/u_T
Tower	398	
-18, 45	334	.839
-18, 35	326	.819
-18, 25	318	.799
-18, 15	276	.693

Run 103, 1125-1135, WD 278°

Position	u_z	u_z/u_T
Tower	349	
-18, 45	302	.865
-18, 35	295	.845
-18, 25	292	.837
-18, 15	255	.731

Run 104, 1825-1835, WD 284°

Position	u_z	u_z/u_T
Tower	682	
-23, 68	331	.485
-23, 60	441	.647
-23, 47	640	.938

Run 105, 1920-1930, WD 294°

Position	u_z	u_z/u_T
Tower	471	
-23, 68	224	.476
-23, 60	306	.650
-23, 47	420	.892

Run 106, 1930-1940, WD 287°

Position	u_z	u_z/u_T
Tower	422	
-23, 68	215	.509
-23, 60	278	.659
-23, 47	376	.891

September 17, 1962

Run 107, 1515-1525, WD 180°

Position	u_z	u_z/u_T
Tower	670	
-26, 49	659	.984
-27, 34	631	.942
-28, 24	622	.928

Run 108, 1530-1540, WD 180°

Position	u_z	u_z/u_T
Tower	675	
-26, 44	667	.988
-27, 34	641	.950
-28, 24	611	.905

September 20, 1962

Run 109, 1055-1105, WD 216°

Position	u_z	u_z/u_T
Tower	854	
-37, 65	542	.635
-37, 55	428	.501
-37, 45	679	.795

Run 110, 1105-1115, WD 215°

Position	u_z	u_z/u_T
Tower	808	
-37, 65	466	.577
-37, 55	414	.512
-37, 45	742	.918

Run 111, 1115-1125, WD 212°

Position	u_z	u_z/u_T
Tower	657	
-37, 65	408	.621
-37, 55	367	.559
-37, 45	641	.976

Run 112, 0950-1000, WD 226°

Position	u_z	u_z/u_T
Tower	729	
-37, 70	381	.523
-37, 60	600	.323
-37, 50	621	.852

Run 113, 1000-1010, WD 222°

Position	u_z	u_z/uT
Tower	758	
-37, 70	409	.540
-37, 60	594	.784
-37, 50	669	.883

Run 114, 1015-1025, WD 221°

Position	u_z	u_z/uT
Tower	761	
-37, 70	410	.539
-37, 60	564	.741
-37, 50	693	.911

September 17, 1962

Run 115, 1700-1710, WD 180°

Position	u_z	u_z/uT
Tower	662	
-48, 44	617	.932
-48, 34	538	.813
-48, 24	437	.660

Run 116, 1725-1800, WD 180°

Position	u_z	u_z/uT
Tower	676	
-48, 44	613	.907
-48, 34	511	.756
-48, 24	467	.691

Run 117, 1800-1810, WD 180°

Position	u_z	u_z/uT
Tower	657	
-48, 44	608	.925
-48, 34	496	.755
-48, 24	481	.732

Run 118, 1810-1820, WD 180°

Position	u_z	u_z/uT
Tower	714	
-48, 44	632	.885
-48, 34	532	.745
-48, 24	454	.636

September 20, 1962

Run 119, 1155-1205, WD 224°

Position	u_z	u_z/uT
Tower	715	
-50, 65	615	.860
-50, 55	382	.534
-50, 45	613	.857

Run 120, 1205-1215, WD 225°

Position	u_z	u_z/uT
Tower	748	
-50, 65	667	.892
-50, 55	411	.549
-50, 45	650	.869

Run 121, 1215-1225, WD 227°

Position	u_z	u_z/uT
Tower	778	
-50, 65	667	.857
-50, 55	424	.545
-50, 45	662	.851

Run 122, 1520-1530, WD 216°

Position	u_z	u_z/uT
Tower	712	
-83, 74	267	.375
-73, 74	268	.376
-63, 74	227	.319
-53, 74	134	.188

Run 123, Position	1530-1540, u_z	WD 210° u_z/u_T
Tower	757	
-83, 74	271	.358
-73, 74	276	.365
-63, 74	222	.293
-53, 74	117	.155

Run 124, Position	1545-1555, u_z	WD 208° u_z/u_T
Tower	751	
-83, 74	254	.338
-73, 74	278	.370
-63, 74	226	.301
-53, 74	116	.154

Run 125, Position	1905-1915, u_z	WD 210° u_z/u_T
Tower	1296	
-75, 97	547	.422
-65, 97	522	.403
-55, 97	474	.366
-45, 97	341	.263

Run 126, Position	1915-1930, u_z	WD 213° u_z/u_T
Tower	1352	
-75, 97	556	.411
-65, 97	543	.402
-55, 97	498	.368
-45, 97	253	.187

Run 127, Position	1925-1935, u_z	WD 214° u_z/u_T
Tower	1253	
-75, 97	550	.439
-65, 97	530	.423
-55, 97	472	.377
-45, 97	348	.278

September 22, 1962

Run 128, Position	1925-1935, u_z	WD 155° u_z/u_T
Tower	842	
-75, 97	229	.272
-65, 97	274	.325
-55, 97	389	.462
-45, 97	422	.501

Run 129, Position	1935-1945, u_z	WD 159° u_z/u_T
Tower	893	
-75, 97	260	.291
-65, 97	332	.372
-55, 97	481	.539
-45, 97	479	.536

Run 130, Position	1945-1955, u_z	WD 159° u_z/u_T
Tower	856	
-75, 97	241	.282
-65, 97	291	.340
-55, 97	429	.501
-45, 97	450	.526

September 23, 1962

Run 131, Position	2320-2330, u_z	WD 190° u_z/u_T
Tower	884	
-75, 97	526	.595
-65, 97	521	.589
-55, 97	419	.474
-45, 97	300	.339

Run 132, Position	2330-2340, u_z	WD 187° u_z/u_T
Tower	883	
-75, 97	501	.567
-65, 97	499	.565
-55, 97	413	.468
-45, 97	289	.327

Run 133, 2340-2350, WD 184°		
Position	u_z	u_z/u_T
Tower	981	
-75, 97	562	.573
-65, 97	521	.531
-55, 97	410	.418
-45, 97	341	.348

Run 137, 1757-1807, WD 180°		
Position	u_z	u_z/u_T
Tower	571	
-42, 116	461	.807
-42, 112	396	.694
-42, 108	336	.588
-42, 104	298	.522
-42, 100	271	.475

August 17, 1962

Run 134, 1648-1658, WD 180°		
Position	u_z	u_z/u_T
Tower	468	
-42, 116	435	.929
-42, 112	428	.914
-42, 108	414	.885
-42, 104	407	.870
-42, 100	380	.812

Run 135, 1659-1709, WD 180°		
Position	u_z	u_z/u_T
Tower	508	
-42, 116	503	.990
-42, 112	512	1.008
-42, 108	499	.982
-42, 104	497	.978
-42, 100	451	.888

Run 136, 1710-1720, WD 180°		
Position	u_z	u_z/u_T
Tower	548	
-42, 116	494	.901
-42, 112	466	.850
-42, 108	427	.779
-42, 104	399	.728
-42, 100	357	.651

September 23, 1962

Run 138, 1410-1420, WD 184°		
Position	u_z	u_z/u_T
Tower	1202	
-42, 140	1210	1.007
-42, 130	1214	1.010
-42, 120	1094	.910
-42, 110	750	.624
-42, 102	852	.709

Run 139, 1420-1430, WD 187°		
Position	u_z	u_z/u_T
Tower	1259	
-42, 140	1262	1.002
-42, 130	1259	1.000
-42, 120	1165	.925
-42, 110	1153	.916
-42, 102	1001	.795

Run 140, 1435-1445, WD 186°		
Position	u_z	u_z/u_T
Tower	1131	
-42, 140	1050	.928
-42, 130	1119	.989
-42, 120	982	.868
-42, 110	465	.411
-42, 102	499	.441

August 17, 1962

Run 141, 1009-1019, WD 180°

Position	u_z	u_z/u_T
Tower	558	
-18, 116	551	.987
-18, 112	531	.952
-18, 108	492	.882
-18, 104	447	.801
-18, 100	406	.728

Run 142, 1020-1030, WD 180°

Position	u_z	u_z/u_T
Tower	578	
-18, 116	571	.988
-18, 112	564	.976
-18, 108	538	.931
-18, 104	509	.881
-18, 100	460	.796

September 23, 1962

Run 143, 1645-1655, WD 190°

Position	u_z	u_z/u_T
Tower	1141	
-1, 140	1124	.985
-1, 130	1146	1.004
-1, 120	1162	1.018
-1, 110	1192	1.045
-1, 102	909	.797

Run 144, 1655-1705, WD 187°

Position	u_z	u_z/u_T
Tower	1133	
-1, 140	1119	.988
-1, 130	1140	1.006
-1, 120	1157	1.021
-1, 110	1185	1.046
-1, 102	1197	1.056

Run 145, 1705-1715, WD 186°

Position	u_z	u_z/u_T
Tower	1134	
-1, 140	1111	.980
-1, 130	1128	.995
-1, 120	1138	1.004
-1, 110	1166	1.028
-1, 102	1190	1.049

Run 146, 1715-1725, WD 186°

Position	u_z	u_z/u_T
Tower	1139	
-1, 140	1145	1.005
-1, 130	1169	1.026
-1, 120	1183	1.039
-1, 110	1218	1.069
-1, 102	943	.828

October 24, 1962

Run A, 1805-1815, WD 215°

Position	u_z	u_z/u_T
Tower	827	
43, 145	800	.968

Run B, 1830-2240, WD 215°

Position	u_z	u_z/u_T
Tower	725	
43, 145	704	.971

October 25, 1962

Run C, 0850-0900, WD 140-180°

Position	u_z	u_z/u_T
Tower	246	
43, 145	245	.999

Run D, 0910-0920, WD 170-150°

Position	u_z	u_z/u_T
Tower	319	
43, 145	316	.991

Run E, 0920-0930, WD 150°

Position	u_z	u_z/u_T
Tower	331	
43, 145	329	.994

Comparison of Observed Wind Velocity Ratios with the Theoretical Velocity Ratios, Argus Island, August-October, 1962

Position*	u_z**	u_z/u_T	$\frac{u_z \text{ obs.}}{u_z \text{ theo.}}$
Run 1-2, WD 180°			
Tower	459		
0, 116	516	1.12	1.20
0, 112	-	.98	1.13
0, 108	421	.92	.98
0, 104	333	.72	.78
0, 100	292	.64	.69
Run 3-7, WD 180°			
Tower	403		
20, 116	444	1.10	1.17
20, 112	454	1.13	1.20
20, 108	437	1.08	1.16
20, 104	326	.81	.87
20, 100	205	.51	.55
Run 8-10, WD 186°			
Tower	1058		
43, 139	999	.94	1.01
43, 129	1007	.95	1.03
43, 119	1006	.95	1.04
43, 109	1051	.99	1.09
43, 101	1100	1.04	1.15
Run 11-16, WD 180°			
Tower	535		
43, 116	501	.94	1.00
43, 112	512	.96	1.02
43, 108	527	.98	1.05
43, 104	540	1.01	1.08
43, 100	510	.95	1.03

Position	u_z	u_z/u_T	$\frac{u_z \text{ obs.}}{u_z \text{ theo.}}$
Run 20-22, WD 201°			
Tower	877		
41, 99	754	.85	.96
61, 99	770	.88	.98
81, 99	788	.90	1.00
Run 23-25, WD 181°			
Tower	772		
75, 95	662	.86	.96
67, 95	642	.83	.93
57, 95	619	.80	.89
47, 95	572	.74	.83
Run 34-40, WD 205-210°			
Tower	852		
76, 82	628	.74	.84
76, 62	666	.78	.91
76, 43	686	.80	.97
76, 33	680	.80	.99
76, 23	655	.77	.99
76, 17	633	.74	1.00
Run 41-44, WD 210-220°			
Tower	862		
66, 82	590	.68	.77
66, 62	629	.73	.85
66, 45	690	.80	.96
66, 33	700	.81	1.01
66, 23	679	.79	1.02
66, 17	641	.74	1.00

* All positions by Cartesian coordinates as in figure 1

** All velocities in cm sec^{-1}

Position	u_z	u_z/u_T	$\frac{u_z \text{ obs.}}{u_z \text{ theo.}}$
Run 45-48, WD 225°			
Tower	738		
57, 82	434	.59	.67
57, 62	546	.74	.86
57, 45	608	.82	.98
57, 33	605	.82	1.02
57, 23	594	.80	1.03
57, 17	558	.76	1.01
Run 64-70, WD 180°			
Tower	445		
52, 69	220	.49	.56
52, 65	316	.71	.82
52, 61	338	.76	.88
52, 57	350	.79	.93
52, 53	352	.79	.93
Run 71-73, WD 232°			
Tower	773		
30, 67	332	.43	.50
30, 57	729	.94	1.10
30, 47	686	.89	1.07
30, 37	674	.87	1.07
Run 74-77, WD 225-247°			
Tower	887		
26, 57	880	.99	1.16
27, 47	809	.91	1.09
28, 37	788	.88	1.08
29, 27	853	.96	1.22
Run 78-85, WD 180-225°			
Tower	912		
30, 17	728	.80	1.07
Run 86-88, WD 233-238°			
Tower	770		
17, 68	401	.52	.60
17, 60	781	1.01	1.18
17, 50	731	.95	1.13
17, 40	680	.88	1.07

Position	u_z	u_z/u_T	$\frac{u_z \text{ obs.}}{u_z \text{ theo.}}$
Run 89-91, WD 275°			
Tower	580		
-10, 53	408	.70	.83
-10, 43	483	.83	1.00
-10, 33	497	.86	1.07
-10, 23	442	.76	.98
Run 92-94, WD 261-274°			
Tower	468		
-10, 63	389	.83	.96
-10, 53	380	.81	.96
-10, 43	327	.70	.84
-10, 33	433	.93	1.15
Run 95-97, WD 262-266°			
Tower	453		
-10, 68	331	.73	.84
-10, 58	400	.88	1.03
-10, 48	321	.71	.85
-10, 38	447	.99	1.21
Run 98-100, WD 242-246°			
Tower	495		
-18, 70	442	.89	1.03
-18, 60	478	.97	1.13
Run 101-103, WD 278-288°			
Tower	433		
-18, 45	368	.85	1.02
-18, 35	368	.85	1.05
-18, 25	354	.82	1.05
-18, 15	309	.71	.97
Run 104-106, WD 284-297°			
Tower	525		
-23, 47	479	.91	1.09

Position	u_z	u_z/u_T	$\frac{u_z \text{ obs.}}{u_z \text{ theo.}}$
Run 107-108, WD 180°			
Tower	673		
-26, 44	663	.99	1.19
-27, 34	632	.94	1.16
-28, 24	617	.92	1.18
Run 109-111, WD 212-216°			
Tower	773		
-37, 65	472	.61	.71
-37, 55	402	.52	.61
-37, 45	687	.89	1.07
Run 112-114, WD 221-226°			
Tower	749		
-37, 70	400	.53	.61
-37, 60	586	.78	.91
-37, 50	661	.88	1.05
Run 115-118, WD 180°			
Tower	677		
-48, 44	618	.91	1.10
-48, 34	519	.77	.95
Run 119-121, WD 224-227°			
Tower	747		
-50, 45	642	.86	1.03
Run 122-124, WD 208-216°			
Tower	740		
-83, 74	264	.36	.41
-73, 74	274	.37	.42
-63, 74	225	.30	.34
-53, 74	122	.16	.18
Run 131-133, WD 184-190°			
Tower	916		
-75, 97	530	.58	.64
-65, 97	514	.56	.62
-55, 97	414	.45	.50
-45, 97	310	.34	.38

Position	u_z	u_z/u_T	$\frac{u_z \text{ obs.}}{u_z \text{ theo.}}$
Run 134-137, WD 180-187°			
Tower	524		
-42, 116	473	.90	.96
-42, 112	451	.86	.92
-42, 108	419	.80	.85
-42, 104	400	.76	.82
-42, 100	365	.70	.75
Run 138-140, WD 184-187°			
Tower	1198		
-42, 140	1174	.98	1.05
-42, 130	1197	1.00	1.08
-42, 120	1080	.90	.98
-42, 110	789	.66	.72
-42, 102	784	.65	.72
Run 141-142, WD 180°			
Tower	568		
-18, 116	561	.99	1.05
-18, 112	546	.96	1.02
-18, 108	515	.91	.97
-18, 104	478	.84	.90
-18, 100	433	.76	.82
Run 143-146, WD 186-190°			
Tower	1137		
-1, 140	1125	.99	1.06
-1, 130	1146	1.01	1.09
-1, 120	1160	1.02	1.11
-1, 110	1190	1.05	1.15
-1, 102	1060	.93	1.03

DISTRIBUTION LIST
FOR
CONTRACT NONR 2997(00), NR 389-101
(Figure in ( ) indicates number of copies distributed to each group)

Chief of Naval Research (2)
Attention Geography Branch
Office of Naval Research
Washington 25, D. C.

Armed Services Tech. Information (10)
Agency
Arlington Hall Station
Arlington 12, Virginia

Director (6)
Naval Research Laboratory
Attention : Technical Information Officer
Washington 25, D. C.

Commanding Officer (1)
Office of Naval Research Branch Office
207 West 24th Street
New York 11, New York

Commanding Officer (1)
Office of Naval Research Branch Office
1030 East Green Street
Pasadena 1, California

Commanding Officer (1)
Office of Naval Research Branch Office
The John Crerar Library Building
86 East Randolph Street
Chicago 1, Illinois

Commanding Officer (12)
Office of Naval Research
Navy #100
Fleet Post Office
New York, New York

Office of Technical Services (1)
Department of Commerce
Washington 25, D. C.

Chief of Naval Research/407 M (1)
Office of Naval Research
Washington 25, D. C.

Chief of Naval Research /Code 407S/ (1)
Office of Naval Research
Washington 25, D. C.

Chief of Naval Research /Code 416/ (1)
Office of Naval Research
Washington 25, D. C.

Chief of Naval Research /Code 461/ (1)
Office of Naval Research
Washington 25, D. C.

Chief of Naval Research /Code 463/ (1)
Office of Naval Research
Washington 25, D. C.

Chief of Naval Operations /OP09B7/ (1)
Department of the Navy
Washington 25, D. C.

Chief of Naval Operations /OP 922 H/ (1)
Department of the Navy
Washington 25, D. C.

Commandant (1)
Marine Corps Schools
Quantico, Virginia

The Oceanographer (1)
U. S. Navy Oceanographic Office
Washington 25, D. C.

Commanding Officer (1)
U.S. Naval Photo Interpretation Ctre
4301 Suitland Road
Washington 25, D. C.

Chief, Bureau of Yards and Docks (1)
Code 70, Office of Research
Department of the Navy
Washington 25, D. C.

President (1)
U. S. Naval War College
Newport, Rhode Island

Officer-in-Charge (1)
U. S. Naval Civil Engineering Research and Evaluation Laboratory
Construction Battalion Center
Port Hueneme, California

Chief, Bureau of Weapons Meteorological Division (1)
Department of the Navy
Washington 25, D. C.

Commander (1)
Air Force Cambridge Research Center
L. G. Hanscom Field
Bedford, Massachusetts

Director, Research Studies Institute (1)
Air University
Attention: ADTIC
Maxwell Air Force Base
Montgomery, Alabama

Headquarters Air Weather Service (1)
Scott Air Force Base
Illinois

Dr. Leonard S. Wilson (1)
Research Branch
R & D Division G-4, DA
Room 3B480, Pentagon
Washington 25, D. C.

Research and Engineering Command (1)
U. S. Army
ATTN: Environmental Protection Division
Natick, Massachusetts

Engineer Intelligence Division (1)
Office of the Chief of Engineers
Gravelly Point, Building T-7
Washington 25, D. C.

Office of the Chief of Engineers (1)
Research and Development Division
Department of the Army
Washington 25, D. C.

Commanding Officer (1)
Army Map Service
6500 Brooks Lane
Washington 25, D. C.

Resident Member (1)
Corps of Engineers, U.S. Army
Beach Erosion Board
5201 Little Falls Road, N. W.
Washington 16, D. C.

Office of Asst. Ch. Staff for Intelligence (1)
Department of the Army
Washington 25, D. C.

Department of the Army (1)
Office, Chief of Transportation
Building T-7
Washington 25, D. C.

U. S. Army Cold Regions Res. & Eng. Lab. (1)
P. O. Box 282
Hanover, New Hampshire

Director, Central Intelligence Agency (2)
Attention: Map Division
Washington 25, D. C.

Commandant (1)
U. S. Coast Guard
Headquarters
Washington 25, D. C.

Office of Geography (1)
Department of the Interior
Washington 25, D. C.

Military Geology Branch (1)
U. S. Geological Survey
Department of the Interior
Washington 25, D. C.

Daniel B. Beard (1)
Chief of Interpretation
National Park Service
Department of Interior
Washington 25, D. C.

U. S. Weather Bureau (1)
Attention: Scientific Services Division
24th and M Street, N. W.
Washington 25, D. C.

Dr. Reid A. Bryson (1)
Department of Meteorology
University of Wisconsin
Madison 6, Wisconsin

Dr. Richard J. Russell (1)
Coastal Studies Institute
Louisiana State University
Baton Rouge 3, Louisiana

Dr. John H. Vann (1)
Department of Geography
Louisiana State University
Baton Rouge 3, Louisiana

Dr. Arthur N. Strahler (1)
Department of Geology
Columbia University
New York 27, New York

Dr. H. Homer Aschmann (1)
Division of Social Science
University of California
Riverside, California

Dr. Charles B. Hitchcock (1)
American Geographical Society
Broadway at 156th Street
New York 32, New York

Dr. Edward B. Espenshade (1)
Department of Geography
Northwestern University
Evanston, Illinois

Professor H. E. Wright, Jr. (1)
Department of Geology and Minerology
University of Minnesota
Minneapolis 14, Minnesota

Dr. David S. Simonett (1)
Department of Geography
University of Kansas
Lawrence, Kansas

Professor J. W. Johnson (1)
Water Resources Center, Archives
University of California
Berkeley 4, California
/U.S. Reports only/

Dr. William L. Garrison (1)
Department of Geography
Northwestern University
Evanston, Illinois

Dr. M. Gordon Wolman (1)
Department of Geography
Johns Hopkins University
Baltimore 18, Maryland

Chief of Naval Research (1)
Code 446
Office of Naval Research
Washington 25, D. C.

Executive Secretary (1)
Environmental Sciences and Engineering
Study Section
Division of Research Grants
National Institutes of Health
Bethesda 14, Maryland

Dr. Robert E. Stevenson (1)
Department of Oceanography & Meteorology
A & M College of Texas
College Station, Texas